KONA Powder and Particle Journal

KONA Powder and Particle Journal No. 41 (2024) 197–220/https://doi.org/10.14356/kona.2024014 Review Paper

Synthesis of Anisotropic Metal Oxide Nanoparticles via Non-Aqueous and Non-Hydrolytic Routes †

Sherif Okeil [1,4], Julian Ungerer [2], Hermann Nirschl [2] and Georg Garnweitner [1,3]*

[1] *Institute for Particle Technology, Technische Universität Braunschweig, Germany*
[2] *Institute for Mechanical Process Engineering and Mechanics, Karlsruhe Institute of Technology (KIT), Germany*
[3] *Laboratory for Emerging Nanometrology, Technische Universität Braunschweig, Germany*
[4] *Pharmaceutical Analytical Chemistry Department, Faculty of Pharmacy, Ain Shams University, Egypt*

Due to their low cost, high stability and low toxicity, metal oxide nanomaterials are widely used for applications in various fields such as electronics, cosmetics and photocatalysis. There is an increasing demand thereby for nanoparticles with highly defined properties, in particular a narrow particle size distribution and a well-defined morphology. Such products can be obtained under high control via bottom-up synthesis approaches. Although aqueous processes are largely found in literature, they often lead to particles with low crystallinity and broad size distribution. Thus, there has been a growing trend towards the use of non-aqueous and non-hydrolytic synthesis routes. Through variation of the reaction medium and the use of adequate additives, such non-aqueous systems can be tuned to adapt the product properties, and especially to yield anisotropic nanoparticles with peculiar shapes and even complex architectures. Anisotropic particle growth enables the exposure of specific facets of the oxide nanocrystal, leading to extraordinary properties such as enhanced catalytic activity. Thus, there is an increasing demand for anisotropic nanoparticles with tailored morphologies. In this review, the non-aqueous and non-hydrolytic synthesis of anisotropic metal oxide nanoparticles is presented, with a particular focus on the different parameters resulting in anisotropic growth to enable the rational design of specific morphologies. Furthermore, secondary phenomena occurring during anisotropic particle growth, such as oriented attachment mechanisms, will be discussed.

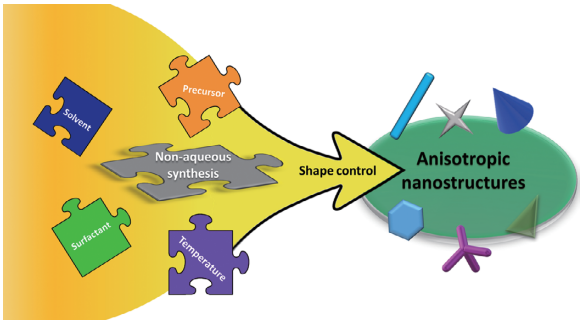

Keywords: non-aqueous synthesis, non-hydrolytic synthesis, anisotropic nanoparticles, metal oxides, oriented attachment

1. Introduction

Metal oxides emerged as an indispensable class of materials due to the wide range of properties they can exhibit according to their composition, degree of crystallinity and morphology. Thus, they are employed in various technological fields such as catalysis (Védrine, 2017), electronics, including transistors (Yu et al., 2016) and gas sensors (Arafat et al., 2012; Chavali and Nikolova, 2019; Yu et al., 2022), as well as energy storage (Ellis et al., 2014; Fleischmann et al., 2022; Su et al., 2016) and solar cells (Chen et al., 2012). These diverse applications of metal oxides often require the use of particles with defined properties. In particular, due to their advantages such as high specific surface area providing high surface activity or small size providing a high degree of homogeneity, nanoparticles of metal oxides are desired. Hence, synthesis routes which enable the synthesis of metal oxides with tailored properties and which at the same time are reliable, cost-effective, versatile and scalable are important prerequisites for many of these applications.

In the past decades, scientists have always been working on different synthesis techniques to access metal oxide nanomaterials. Therefore, various synthesis methods exist, ranging from top-down methods such as ball milling and laser ablation to bottom-up methods like gas-phase synthesis and solution-based methods (Chavali and Nikolova, 2019; Parashar et al., 2020). While gas-phase synthesis is often expensive and requires large instrumentation, the solution-based synthesis of metal oxide nanoparticles is simple, comparatively less expensive, easily scalable and still enables precise control of the formed nanoparticles. To date, the solution-based synthesis of metal oxides is carried out mainly via aqueous synthesis, although non-aqueous and non-hydrolytic synthesis routes offer interesting advantages for nanoparticle synthesis.

In the case of aqueous synthesis, the precursor compound—which often is a metal alkoxide or other reactive metal compound—reacts with water directly in a hydrolysis step. This usually results in very high reaction rates,

† Received 7 September 2022; Accepted 4 May 2023
J-STAGE Advance published online 31 August 2023
* Corresponding author: Georg Garnweitner;
[1] Add: Volkmaroder Str. 5, 38104 Braunschweig, Germany
[3] Add: Langer Kamp 6A, 38106 Braunschweig, Germany
E-mail: g.garnweitner@tu-braunschweig.de
TEL: +49 (531) 391-65371 FAX: +49 (531) 391-9633

which decreases the homogeneity of the resulting product and leads to difficulty in adjusting or controlling the product properties (Chang and Doong, 2006). Many reaction parameters such as the rate of addition of precursor or water, the type and intensity of mixing, as well as solution parameters like pH, ionic strength, the type and concentration of chelating agents must be precisely controlled to obtain reproducible results. Concerning crystallinity of the resulting nanoparticles, the aqueous sol-gel synthesis at low temperatures usually results in amorphous or low-crystallinity oxides, and requires further heat treatment of the obtained product to obtain crystallinity (Wu et al., 2007a; Zhang et al., 2005). However, calcination at high temperatures results in an increase of crystallite size, neck formation and thus aggregate formation, and eventually even decomposition or phase transformation (Satapathy et al., 2014; Wang et al., 2002). In contrast, in the non-aqueous or non-hydrolytic synthesis, highly crystalline metal oxides are obtained directly in many cases (Wang et al., 2005). Moreover, the crystal phase can even be tuned by varying the reaction conditions of the non-aqueous synthesis (Wu et al., 2007a). This makes the non-aqueous and non-hydrolytic synthesis an attractive pathway for the simplified production of certain nanomaterials (Buonsanti et al., 2008; Niederberger and Garnweitner, 2006).

In non-aqueous synthesis routes, no water is added to the reaction mixture. Usually, an organic solvent is employed as a reaction medium but it can also act as a stabilizing agent, which results in a simpler reaction procedure and enables the synthesis of nanomaterials with uniform properties and a lower amount of strongly bound organics due to the absence of surfactants in the case of solvent-directed syntheses (Mutin and Vioux, 2013; Niederberger and Pinna, 2009). In contrast, the synthesis of nano-sized particles in aqueous media often requires the addition of various surfactants and capping agents that limit the growth of the inorganic particles and stabilize the resulting dispersion. While enabling a precise control over the resulting shape and particle size distribution, this also leads to coverage of the surface of the resulting particles by a large amount of surface organics (Niederberger and Pinna, 2009). In non-aqueous synthesis, alcohols are often used as reaction media, and water may be formed in situ during the synthesis process. On the other hand, non-hydrolytic synthesis proceeds in the absence of hydroxyl groups and thus requires the use of an aprotic medium.

In the past few decades, there was an immense increase of interest in crystal engineering, where a huge spectrum of anisotropic particle shapes has been reported for nanoparticles of different materials (Görke and Garnweitner, 2021). A general classification of nanomaterials can be made according to their dimensionality into one-dimensional nanostructures, like nanorods and nanowires, two-dimensional nanostructures such as nanoplatelets and sheet-like structures, and finally more complex three-dimensional nanostructures such as nanocubes, nanopyramids, nanostars, tetrapods or multipods. Small nanoparticles, in contrast, are often referred to as zero-dimensional nanodots. Each of these morphologies can lead to distinct anisotropic properties which are in most cases unique and make them suitable for specific applications rather than spherical nanoparticles which lack the direction-dependent properties (Burrows et al., 2016; Sajanlal et al., 2011). For example, the exposure of specific crystal planes was found to have a drastic effect on the photocatalytic efficiency of metal oxide nanoparticles (Chang and Waclawik, 2012). Anisotropic iron oxide nanoparticles show magnetic behavior which is highly dependent on its shape anisotropy, resulting in enhanced performance in different biomedical applications (Andrade et al., 2020). Metal oxide nanotube structures expose outer and inner surfaces as well as edges, which results in an increased surface area that proved to be highly beneficial for energy storage applications and can be used to embed other materials to form nanocomposites (Ellis et al., 2014; Patzke et al., 2002). All this shows the importance of anisotropic metal oxide nanoparticles. Generally, anisotropic shapes can be formed either through seed-mediated growth which usually results in monocrystalline nanoparticles, through oriented attachment or controlled aggregation (Burrows et al., 2016). Interestingly, non-aqueous synthesis routes can feature chemical species formed in situ that can direct anisotropic growth (Djerdj et al., 2008a) or even form inorganic-organic hybrid nanostructures through self-assembly (Pinna and Niederberger, 2008). Thus, the non-aqueous or non-hydrolytic synthesis routes show a high potential in obtaining anisotropic shapes in a simple manner.

Understanding the formation mechanisms of metal oxide nanoparticles is crucial for predicting anisotropic growth and enabling the rational design of new non-aqueous synthesis routes capable of producing such anisotropic shapes. There are several review articles (Deshmukh and Niederberger, 2017; Jun et al., 2006; Mutin and Vioux, 2013, 2009; Niederberger and Garnweitner, 2006; Niederberger and Pinna, 2009; Pinna and Niederberger, 2008; Styskalik et al., 2017) presenting the different non-aqueous or non-hydrolytic synthesis routes for metal oxides and discussing the reaction mechanisms leading to particle formation. Additionally, several general reviews have been published on the wet chemical synthesis of metal oxide nanoparticles (Jun et al., 2006; Nikam et al., 2018) or their applications (Chavali and Nikolova, 2019; Yu et al., 2016). In contrast to these, this contribution will be limited to the synthesis of anisotropic metal oxides in non-aqueous and non-hydrolytic systems. In this way, we aim to provide a deeper insight into the formation of anisotropic metal oxide nanoparticles or nanostructures, and discuss the different factors and mechanisms involved in the emergence

of anisotropic particle shapes in the different non-aqueous and/or non-hydrolytic reaction systems. This should help in the design of new tailored non-aqueous synthesis routes for anisotropic metal oxide nanoparticles.

In the following paragraphs, an overview of the synthesis of anisotropic particles of the most important metal oxides via non-aqueous and/or non-hydrolytic synthesis routes will be presented. Each oxide is discussed separately as the interaction of the different solvents and surfactants with the nanocrystal surface differs according to the crystal properties of the metal oxide. This will be followed by a discussion of the unique mechanisms, especially oriented attachment, encountered in the formation of anisotropic metal oxides in non-aqueous and non-hydrolytic synthesis routes. Then, the formation of anisotropic metal oxides in some special solvents, like benzyl alcohol is reviewed. The review is finally concluded by an outlook on possible future directions.

2. Titanium dioxide

The synthesis of titanium dioxide as the most-used photocatalytic material has been the focus of research for decades (Liu et al., 2014). Many studies were devoted to the synthesis of TiO_2 nanoparticles with distinct morphologies due to the increased surface-to-volume ratio where the increased interface permits enhanced catalytic activity (Fattakhova-Rohlfing et al., 2014). **Table S1** in the supplementary material provides a list of non-aqueous and non-hydrolytic synthesis approaches resulting in different anisotropic TiO_2 nanocrystal morphologies in chronological order of their publication. The main factors affecting the anisotropic growth in non-aqueous systems will be discussed in the following text. Although the main factors are presented, it must be considered that interconnections between the different factors exist, which makes it hard to isolate the effect of single factors completely.

2.1 Effect of solvent

Non-aqueous sol-gel synthesis routes were shown as being capable of controlling the size and shape, thus achieving different anisotropic TiO_2 structures with simple one-pot synthesis by simply changing the solvent used. The first non-aqueous synthesis procedure to well-defined anisotropic titania particles was reported by Wang et al., using titanium tetrachloride ($TiCl_4$) as the precursor in a solvent mixture of absolute ethanol and acetic acid (Wang et al., 2001). In this work, different organic solvent mixtures were tested for the synthesis of titania nanoparticles, with only the combination of absolute ethanol with acetic acid yielding anisotropic rutile titania structures (tenuous fiber and rod-like structures, **Table S1**). Ethylene glycol or glycerol as alternatives for ethanol yielded spherical nanoparticles, which was evident from the corresponding TEM and XRD analysis. The authors suggested that the titania formation in these systems mainly proceeds via a hydrolytic mechanism due to the water formed in the system from the esterification reaction between ethanol and acetic acid. The use of solely ethanol as a solvent also resulted in isotropic nanoparticles (Wang et al., 2001; 2002). The difference in the obtained morphologies by changing the alcohol type was rationalized by the preferential surface binding of the ethanol molecules to specific lattice planes, slowing down their growth (Doxsee et al., 1998). The investigation of a series of other alcohols as solvents for the non-aqueous synthesis of titania from $TiCl_4$ at a low temperature showed that fibrous structures could also be obtained in the case of using isopropanol and *n*-butyl alcohol as solvents (Wang et al., 2002).

2.2 Effect of precursor concentration (precursor-to-solvent ratio)

Investigating the influence of the precursor concentration, it was found that the $TiCl_4$/butanol ratio plays an important role in determining the phase and morphology of the formed TiO_2 nanocrystals. Only a low $TiCl_4$/butanol ratio resulted in the formation of rutile-phase nanorods, while higher ratios resulted in isotropic particles (Cao et al., 2011). While the sol-gel reaction of titanium tetrachloride and benzyl alcohol normally yields spherical particles (Niederberger et al., 2002a), nanorod particles have been obtained by Abazović et al. (Abazović et al., 2006; 2008) using the same reaction system, which underlines the importance of the applied reaction conditions. The formation of anatase TiO_2 nanorods in this reaction system has been attributed to the prolonged aging time at an elevated temperature (75 °C for 3 days) , which is longer than that used for spherical particles (24 h only at 75 °C). Rutile-phase TiO_2 nanofibers were also synthesized in a non-aqueous system from $TiCl_4$ in acetone at 110 °C, where the ratio of the precursor to acetone was found to be crucial for tuning the phase and morphology of the synthesized TiO_2. A 1:10 ratio of precursor to acetone was required to obtain rutile-phase nanofibers, while lower precursor concentrations resulted in anatase-phase isotropic and irregular-shaped particles (Wu et al., 2007a; 2007b). The same behavior was also observed with other ketones like butanone, 4-methylpentanone, and acetophenone (Wu et al., 2007b). In contrast, the reaction of titanium isopropoxide in ketones generally results in spherical anatase nanoparticles (Garnweitner et al., 2005).

2.3 Effect of surfactants

While it is evident that changing the solvent can control the morphology of the resulting metal oxide, the addition of a surfactant can further tune and direct the nanoparticle growth and can be used to obtain new particle shapes. Surfactants can preferentially bind to certain facets of a crystal changing its surface-free energy and thus changing

the growth rate of the different facets resulting in anisotropic growth (Bakshi, 2016). Alivisatos et al. used two different surfactants, namely lauric acid (LA), which selectively binds to the anatase {001} facets, and trioctylphosphine oxide (TOPO), which nonselectively coordinates to the TiO_2 surface. By variation of the ratio of these surfactants, it is possible to obtain different anisotropic TiO_2 particles ranging from bullet-shaped and rod-shaped nanocrystals to more complex branched nanocrystal shapes (Jun et al., 2003). At low LA concentrations, anisotropic crystal growth along the [001] direction takes place, eliminating the {001} faces and exposing {101} faces forming bullet-shaped (**Fig. 1(a)**) and diamond-shaped (**Fig. 1(b)**) nanocrystals. Increasing the amount of the LA surfactant slows down the growth along the [001] direction, leading to the formation of facetted nanorods (**Fig. 1(c)** and **(d)**). At very high LA concentrations, further inhibition of the growth in the [001] direction favors the growth of the {101} crystal faces and results in the branching-out of the {101} faces, yielding branched nanorod structures (**Fig. 1(e)**) (Jun et al., 2003).

The use of oleic acid as a surfactant in the non-aqueous titania synthesis in anhydrous toluene yielded dumbbell-shaped nanorods at 250 °C only when the amount of titanium isopropoxide (TIP) precursor was high, using a constant surfactant/precursor ratio of 3:1. At lower precursor concentrations, an increase of the surfactant/precursor ratio above 3:1 was necessary to obtain the dumbbell-shaped nanorods (Kim et al., 2003). This shows that not only the surfactant/precursor ratio is crucial for obtaining anisotropic structures but also the relative amount of precursor to the non-aqueous solvent used.

A reaction of TIP with oleic acid at lower temperatures (80 °C) results in the derivatization of the titanium precursor forming a titanium oleate complex. This can be used as an alternative precursor for the TiO_2 synthesis due to its lower reactivity, which can enable better control of the nanoparticle formation. Adapting the chemical reactivity of the precursor, further control of the nanoparticle synthesis can be achieved. The injection of oleylamine into the non-coordinating solvent 1-octadecene at 260 °C starts the decomposition of the titanium oleate complex through aminolysis, resulting in the formation of TiO_2 which is capped by carboxylate ions. The higher reactivity of the (001) planes leads to the facilitated aminolysis of the capping oleate at these planes, which enables anisotropic growth of the titania nanocrystals in the [001] direction. Thus, titania nanorods are formed whose length can be easily tuned through variation of the injected oleylamine amount. An increase in the oleylamine amount from 1 to 2 mmol increases the titania nanorod length in this system. A further increase was found to suppress anisotropic growth where 3 mmol oleylamine leads to a decrease in the resulting nanorod length; finally for 4 mmol oleylamine, isotropic titania nanoparticles were achieved. The observed suppression of anisotropic growth could be due to the accelerated aminolysis and increased consumption of surface-coordinated oleate by the high oleylamine concentration. Even the diameter of the titania nanorods formed could be tuned in this system through the use of the more weakly binding surfactant cetyltrimethylammonium bromide (CTAB) (Zhang et al., 2005). Thus, variation of the oleylamine/oleic acid ratio represents a powerful tool to tune the morphology of titania nanocrystals.

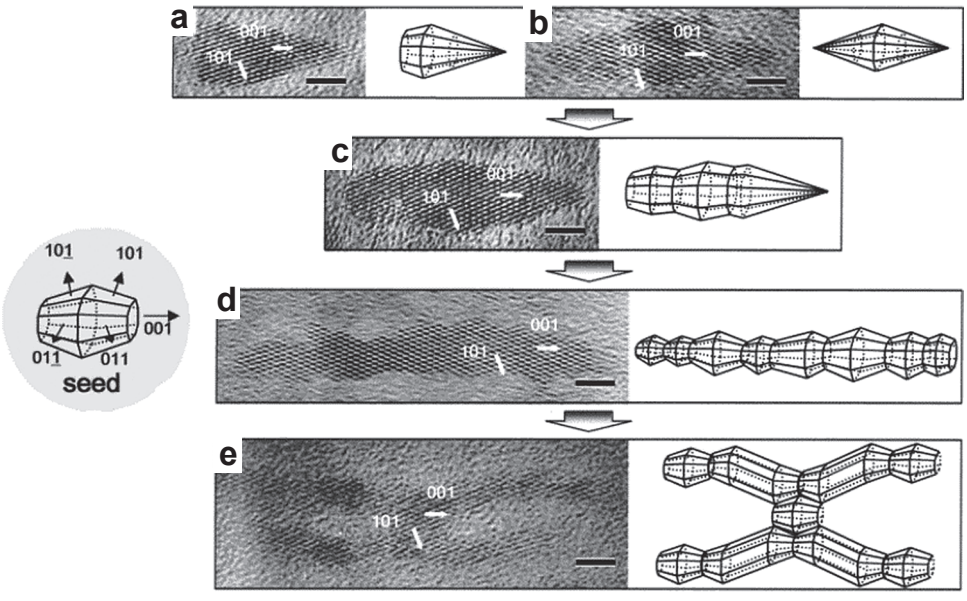

Fig. 1 High-resolution TEM images showing the evolution of different shapes of TiO_2 with varying relative ratio of LA and TOPO surfactants: **(a)** bullet-shaped, **(b)** diamond-shaped, **(c)** short nanorod, **(d)** long nanorod and **(e)** branched nanorod structures (Scale bar = 3 nm). Adapted with permission from Ref. (Jun et al., 2003). Copyright 2003 American Chemical Society.

Through variation of the oleylamine/oleic acid ratio it is also feasible to finely control the shape of the obtained nanorods. Buonsanti et al. observed that at a lower oleylamine/oleic acid ratio of 26, brookite-phase TiO_2 nanorods with tapered tips were obtained, whereas at much higher ratios of about 104, rectangular endings of the TiO_2 nanorods were observed (Buonsanti et al., 2008). It has to be noted that the precursor used is $TiCl_4$ instead of TIP and a seeded-growth technique has been adopted for the synthesis.

A similar system was used by Hyeon et al. for the large-scale non-aqueous synthesis of TiO_2 nanorods, where the TIP precursor was allowed to react with oleic acid at 270 °C for 2 hours, assuming that an ester elimination reaction results in the formation of the titania nanorods growing along the [001] direction (**Fig. 2(a)**). The addition of controlled amounts of 1-hexadecylamine (HDA) enabled control of the resulting nanorod diameter as, according to the authors, HDA strongly coordinates to the (101) anatase faces slowing down its growth. Thus, an increase of the HDA amount leads to a decrease in the titania nanorod diameter from 3.4 nm to 2.0 nm (Joo et al., 2005b). Although it was noted by Zhang et al. that the use of oleic acid or oleylamine alone did not result in particle formation (Zhang et al., 2005), the reaction system of Joo et al. enabled the formation of particles by solely reacting TIP with oleic acid (Joo et al., 2005b).

It was also feasible to obtain ultrathin TiO_2 nanosheets upon heating of $TiCl_4$ precursor in oleylamine alone, which in this case serves as both the solvent and surfactant (**Fig. 2(b)**) (Yang et al., 2015). This shows that the concentration of the precursor and surfactant plays an important role in the particle formation, along with the reaction temperature and synthesis time. It is noteworthy that the synthesis of TiO_2 in oleic acid results in preferential growth in the [001] direction, resulting in nanorods (**Fig. 2(a)**) (Joo et al., 2005b), while the synthesis in oleylamine results in an inhibition of the growth in the [001] direction (*c*-axis) where the preferred growth along the *a*- and *b*-axis yields in the formation of nanosheets (**Fig. 2(b)**) (Yang et al., 2015), which could indicate the different roles of these surfactants.

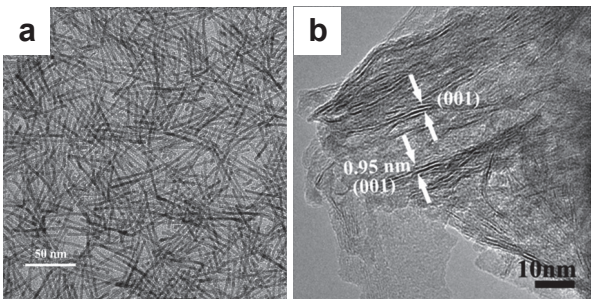

Fig. 2 TEM images of **(a)** TiO_2 nanorods synthesized in oleic acid (adapted with permission from Ref. (Joo et al., 2005b). Copyright 2005 American Chemical Society) and **(b)** ultrathin TiO_2 nanosheets synthesized in oleylamine (adapted with permission from Ref. (Yang et al., 2015). Copyright 2015 The Royal Society of Chemistry).

Detailed investigations of the parameters leading to the anisotropic growth of TiO_2 nanocrystals using a solvothermal synthesis in cyclohexane with titanium butoxide as a precursor and linoleic acid as a surfactant at a low temperature (150 °C for 48 h) were performed by Li et al. The influence of surfactant amount, reaction temperature, reaction time and type of surfactant were studied, where an increase in surfactant amount promoted the anisotropic growth. The nanorods formed also showed spherical tips similar to the dumbbell-shaped nanorods previously obtained in the work by Kim et al. (2003). GC-MS analysis determined the side products formed during the solvothermal synthesis, which indicated an ester elimination reaction mechanism. Checking the effect of carboxylic acid surfactants revealed that ester elimination alone is not sufficient for particle formation; a long-chain organic acid is also crucial for TiO_2 particle formation (Li et al., 2006).

2.4 Effect of doping and precursor addition rate

Alkyl halide elimination for the synthesis of Zr-doped TiO_2 nanocrystals, using a non-hydrolytic, non-aqueous synthesis route, was adopted by using a mixture of a metal halide and a metal alkoxide. TOPO was used as the coordinating solvent. The formation of anisotropic facetted Zr-doped TiO_2 nanorods was only possible at high temperatures (400 °C), with an increase in Zr-doping leading to a subsequent enlargement of the nanorods (Chang and Doong, 2006). The same titania precursors also yielded anisotropic structures at a lower temperature of 300 °C in the non-coordinating solvent 1-octadecene when using oleylamine as the surfactant. The morphology and even the phase of the evolving TiO_2 nanostructures could be precisely controlled through the slow addition of the precursors to hot oleylamine via a syringe pump. A comparably high injection rate of 30 mL/h of the precursors yielded anatase TiO_2 nanorods of 6 nm in diameter and 50 nm in length (**Fig. 3(a)**). Lowering the precursor addition rate to 2.5 mL/h enables the formation of larger anatase nanorods of 9 nm in diameter and 100 nm in length together with rutile-phase star-shaped nanostructures (25 × 200 nm in dimension) (**Fig. 3(b)**). Reducing the flow rate to 1.25 mL/h yields pure rutile star-shaped TiO_2 of 25 nm × 450 nm in size (**Fig. 3(c)**). Consequently, a slower precursor addition rate enabled the formation of fewer nuclei which continuously grew with continuous precursor addition. In contrast, one-shot injection of these precursors into the hot oleylamine resulted in the formation of a mixture of polydisperse nanoparticles and nanorods, which underlines the importance of the addition rate of the precursors in controlling particle morphology (Koo et al., 2006).

3. Zinc oxide

Zinc oxide, as a relatively cheap and non-toxic semiconductor with a wide range of functional properties, has attracted broad attention in various application fields such as gas sensing, piezoelectric devices, photocatalysis, optoelectronic devices and even biomedicine (Bharat et al., 2019; Kolodziejczak-Radzimska and Jesionowski, 2014; Zhang et al., 2013). In all of these applications, shape control can open the door for better integration of ZnO nanostructures into the selected application to reach the desired outcome. Using non-aqueous and non-hydrolytic synthesis routes, unique morphologies such as teardrop-like shape (Zhong and Knoll, 2005), hexagonal pyramid shape (Choi S.H. et al., 2005) and nanowires (Yuhas et al., 2006) were achieved. Supplementary **Table S2** lists the different ZnO particle shapes reported to be obtained from non-aqueous and non-hydrolytic synthesis routes in chronological order of their publication. In the following paragraphs, the effects of different factors on ZnO particle morphology will be discussed in more detail.

3.1 Effect of solvent

Through the use of solvents with different coordinating powers, it was possible to control the shape of evolving ZnO nanoparticles. Thin zinc oxide nanorods (2 nm in diameter) were obtained in trioctylamine (TOA) with oleic acid as a surfactant. The self-assembly of the synthesized nanorods in stacks was observed in this system, with the nanorods being arranged parallel to each other (**Fig. 4(a)**) (Andelman et al., 2005; Yin et al., 2004). The use of the less coordinating solvent 1-hexadecanol (HD) resulted in the formation of less elongated ZnO nanoparticles in the form of nanotriangles (**Fig. 4(b)**). Using the non-coordinating solvent 1-octadecene (OD) results in the loss of anisotropic growth, yielding spherical ZnO nanoparticles (**Fig. 4(c)**) (Andelman et al., 2005). Thus, the choice of solvent, in combination with the surfactant, played an important role in stabilizing the different crystal planes and determining the resulting nanoparticle morphology.

Zhang et al. also tested the influence of different non-coordinating and coordinating solvents on the morphology of the evolving ZnO nanoparticles formed from zinc carboxylate precursors using oleylamine as reagent and surfactant. It is interesting to note that in this work, when employing oleylamine as both a reagent and surfactant, the use of non-coordinating solvents such as dioctyl ether,

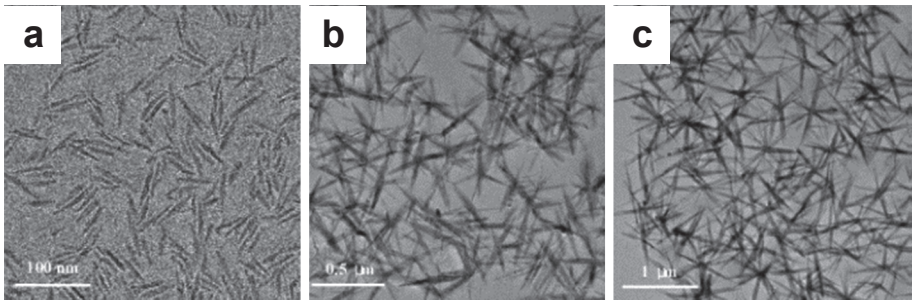

Fig. 3 TEM images of **(a)** anatase TiO_2 nanorods formed at 30 mL/h, **(b)** mixture of anatase nanorods and rutile star-shaped TiO_2 structures formed at 2.5 mL/h and **(c)** pure star-shaped rutile TiO_2 formed at 1.25 mL/h precursor addition rate. Adapted with permission from Ref. (Koo et al., 2006). Copyright 2006 American Chemical Society.

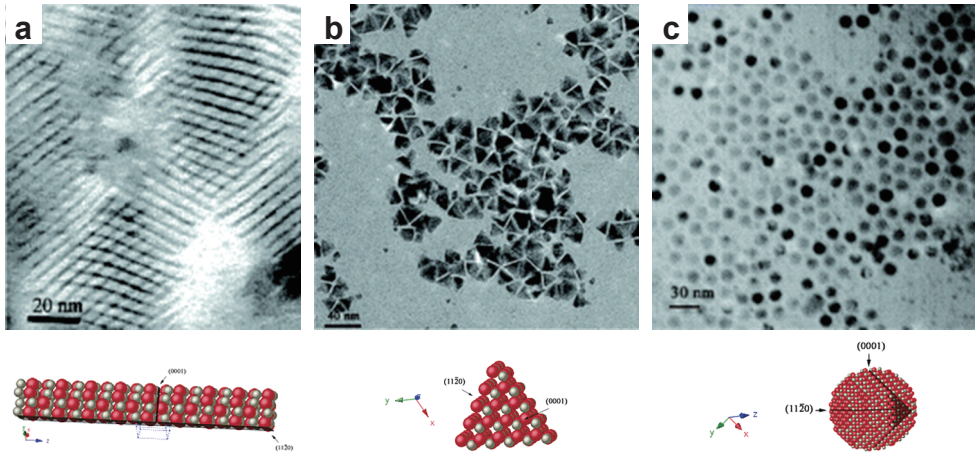

Fig. 4 TEM images with the corresponding crystal structures of **(a)** ultrathin ZnO nanorods self-assembled in stacks, **(b)** ZnO nanotriangles and **(c)** spherical ZnO nanoparticles formed in solvents with different coordinating power. Adapted with permission from Ref. (Andelman et al., 2005). Copyright 2005 American Chemical Society.

diphenyl ether and OD yielded ZnO nanorods (Zhang Z. et al., 2006), which shows that the control of anisotropic growth is a complex interplay between different factors, including the combination of solvent and surfactant used. In this particular system, the use of the coordinating solvent trioctylphosphine (TOP) led to the formation of nanotetrahedrons, similar to the nanotriangles obtained in the work of Andelman et al. (Andelman et al., 2005; Zhang Z. et al., 2006). Increasing the coordinating power by using TOPO as a solvent results in the formation of irregularly shaped particles, which was attributed to the very strong coordination of TOPO to the zinc acetate precursor and the steric effect of the bulky alkyl chains hindering the access for oleylamine to the nanocrystal surface, thus drastically decreasing the kinetics of the aminolytic reaction essential for particle growth in this system (Zhang Z. et al., 2006).

It also has to be mentioned that the role of solvent and surfactant cannot be separated as the solvent itself usually shows some coordination and thus surface activity in covering certain facets of the evolving nanocrystal.

A study of the effect of solvent alone was conducted by Kunjara Na Ayudhya et al., where the influence of different glycols, alcohols, *n*-alkanes and aromatic solvents on the morphology of ZnO nanoparticles was investigated (Kunjara Na Ayudhya et al., 2006). The formation of ZnO from the zinc acetate precursor in glycols and alcohols was achieved at 250 °C, while in non-polar and non-coordinating solvents (*n*-alkanes and aromatic solvents), the precursor decomposition temperature increased to 300 °C. The decomposition temperature of the zinc acetate precursor in the corresponding solvent was related to the dielectric constant of the latter. When the highly polar glycols were used as a solvent, low anisotropic particles of polyhedral shape were obtained, while alcohols yielded nanorods of moderate aspect ratio. The use of *n*-alkanes and aromatic solvents resulted in nanorods with a high-aspect ratio (Kunjara Na Ayudhya et al., 2006). Thus, the aspect ratio of the ZnO nanorods formed was found to be tunable depending on the polarity of the solvent used: the higher the polarity of the solvent, the less the preferential growth of ZnO in the [001] direction. Thus, alcohols with increasing chain length resulted in an increase of the aspect ratio of the ZnO nanorods formed (Cheng and Samulski, 2004; Kunjara Na Ayudhya et al., 2006; Rai et al., 2013; Tonto et al., 2008). Similar observations were made when benzyl alcohol was replaced by the non-polar anisole as a solvent in ZnO synthesis from zinc acetate, where a substantial increase in the nanorod aspect ratio could be observed (Clavel et al., 2007). Other studies reported similar but still deviating behavior using a different precursor and different reaction conditions (Ramya et al., 2019; Šarić et al., 2019). The synthesis of ZnO nanoparticles through a precipitation reaction from zinc acetate and sodium hydroxide in a series of alcohols at low temperatures resulted in isotropic nanoparticles in methanol, mixed nanoparticles and short nanorods in ethanol and nanorods with increasing aspect ratio from butanol to octanol. In octanol, isotropic particles were also observed together with the high-aspect-ratio nanorods. Finally, isotropic particles were obtained again in decanol. In this system, the growth behavior was found to be related to the zeta potential of the formed colloids, which results in different aggregation rates where a lower zeta potential increases the aggregation rate of the colloid and leads to an increased growth rate (Šarić et al., 2019).

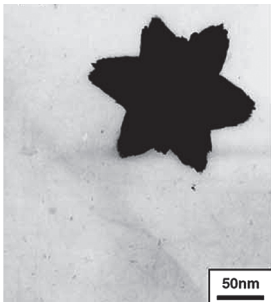

Fig. 5 TEM image of a ZnO nanostar formed from zinc acetate in a mixture of ethanol and ethylene glycol at 80 °C. Adapted with permission from Ref. (Wang et al., 2005). Copyright 2005 Elsevier.

Solvent mixtures are also capable of producing interesting anisotropic structures through selectively enhancing or retarding the growth of specific crystal planes. For example, a mixture of ethanol and ethylene glycol resulted in the formation of ZnO nanostars from a zinc acetate precursor at a low temperature (80 °C) without the need for a surfactant, as can be seen in **Fig. 5** (Wang et al., 2005). In this case, the anisotropic structure formed could be an aggregate of smaller primary particles which possibly resulted in a hierarchical structure, which, however, was not investigated in this work.

3.2 Effect of surfactant and reaction temperature

The ester elimination reaction, similar to that used for the large-scale synthesis of TiO_2 nanorods, has also been applied for the synthesis of different ZnO nanoparticles. The Hyeon Group demonstrated thereby that the use of different surfactants resulted in strong changes in morphology. TOPO, OA, HDA and TDPA in dioctyl ether as solvents resulted in the formation of wedge-shaped ZnO nanocones self-assembled in spherical nanostructures (**Fig. 6(a)**), cone-shaped ZnO nanocrystals (**Fig. 6(b)**), hexagonal cone-shaped ZnO nanocrystals (**Fig. 6(c)**) and ZnO nanorods (**Fig. 6(d)**), respectively (Joo et al., 2005a). Changing the alcohol used to 1,2-dodecanediol and the solvent to the higher-boiling-point-solvent benzyl ether to perform the synthesis at higher temperatures while using TOPO as the surfactant yielded similarly pyramidal or cone-shaped particles (Kachynski et al., 2008).

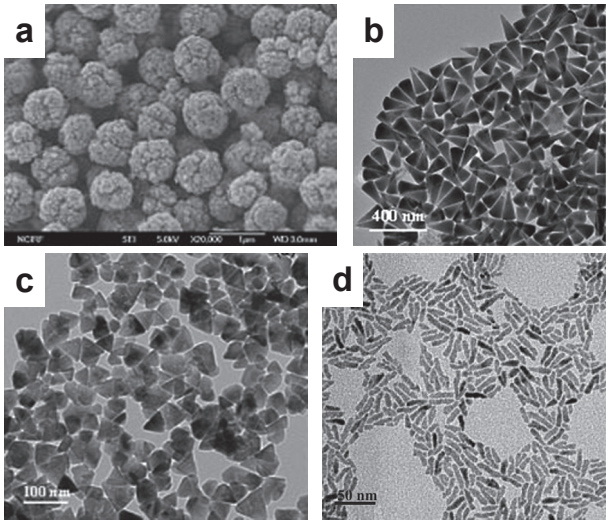

Fig. 6 TEM micrographs of **(a)** spherical hierarchical structures composed of wedge-shaped ZnO nanocones synthesized using TOPO, **(b)** ZnO nanocones synthesized using oleic acid, **(c)** hexagonal ZnO nanocones synthesized using HAD and **(d)** ZnO nanorods synthesized using TDPA as surfactant. Adapted with permission from Ref. (Joo et al., 2005a). Copyright 2005 Wiley-VCH.

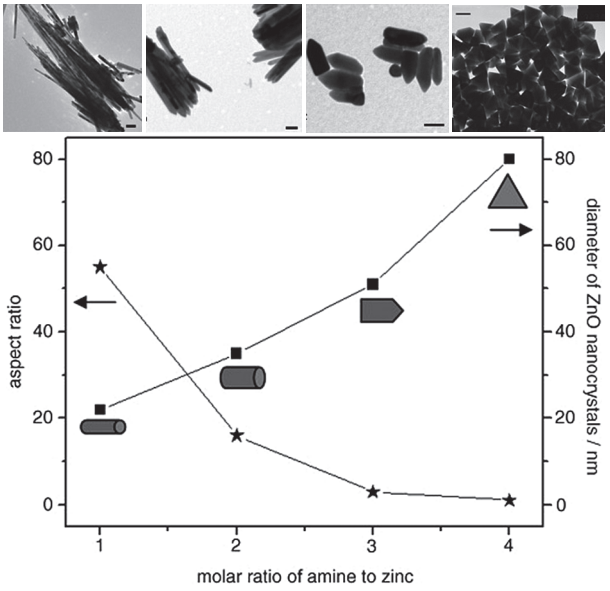

Fig. 7 Diagram showing the relation between the molar ratio of oleylamine to zinc acetate used and the resulting aspect ratio as well as the diameter of the ZnO nanocrystals. Above, for each morphology in the diagram (long nanorods, short nanorods, bullet-shaped nanocrystals and nanoprisms), the corresponding TEM image proving the formation of such ZnO nanomaterial is shown (scale bar: 100 nm). Adapted with permission from Ref. (Zhang et al., 2007). Copyright 2007 Wiley-VCH.

Increasing the concentration of the surfactant also has an influence on the particle shape and can even result in the self-assembly of anisotropic particles to various complex nanostructures. For example, a rise in the concentration of oleylamine used in the synthesis of ZnO in TOP led to the formation of nanotetrahedrons that self-assembled into so-called nanofans. A further increase in the oleylamine concentration resulted in larger dumbbell-shaped nanostructures (Zhang Z. et al., 2006).

The decomposition of zinc acetylacetonate ($Zn(acac)_2$) in oleylamine, which in this case had the role of solvent and surfactant, yielded different particle shapes by varying the oleylamine/precursor molar ratio together with the reaction time and temperature. A ratio of 10:1 at a reaction temperature of 205 °C for 1 h yielded short nanorods arranged in belt-like structures. A lower precursor concentration (ratio 100:1 of oleylamine/precursor) resulted in heart-shaped nanoparticles at 205 °C for 24 h (Liu et al., 2007).

Similarly, the influence of oleylamine on the particle morphology was also investigated by Zhang et al., however, using zinc acetate as the precursor. In this system, the amine was able to attack the precursor in an amide elimination reaction or aminolysis yielding ZnO. In that case, it was found that increasing the molar ratio of oleylamine to precursor decreases the anisotropic growth along the [001] direction, leading to the formation of nanorods with a lower aspect ratio and finally nanoprisms in the case of ratios greater than 3 (**Fig. 7**). A further increase of the oleylamine/precursor ratio up to 24:1 had no significant effect on the resulting morphology (Zhang et al., 2007). It has to be noted that in this work, the precursor used is different, which affects the rate of monomer generation and partly explains the difference to the shapes obtained in the work by Liu et al. (2007). Nevertheless, both works showed a decrease in anisotropic growth with an increasing amount of oleylamine (Liu et al., 2007; Zhang et al., 2007), which was related to an increased reaction rate, leading to rapid nucleation and leaving fewer monomers available for further particle growth. On the other hand, a low amine-to-precursor ratio resulted in a low reaction rate, leading to the formation of fewer initial nuclei and leaving more monomers for further particle growth, where the growth of faster-growing planes becomes apparent, forming highly anisotropic nanocrystals (Zhang et al., 2007).

The testing of other amines (hexadecylamine, dioctylamine and dodecylamine) showed that the longer the alkyl chain of the amine used, the thinner and longer are the ZnO nanowires or nanorods produced when all other reaction parameters are kept constant (Zhang et al., 2007). Correlating these results with other studies where the effect of the solvent was investigated (Clavel et al., 2007; Kunjara Na Ayudhya et al., 2006), it can be deduced that the amines with longer-chain lengths result in higher aspect ratios due to their lower polarity. Using other amines like benzylamine as a reagent to initiate the aminolysis reaction of zinc acetate in benzyl ether also resulted in different anisotropic shapes such as nanocones, nanobullets, nanorods and nanoplates depending on the molar ratio of benzylamine to the zinc precursor as well as the reaction temperature used (Ahmad et al., 2013; Chang and Waclawik, 2012). By

adjusting the amount of benzylamine and the reaction temperature, the reaction rate was controlled which resulted in different nucleation and growth mechanisms. It was found that zinc acetate does not decompose in pure benzyl ether at temperatures below 210 °C unless a reagent initiating an aminolysis reaction is added. Thus, performing a reaction at 170 °C using a benzylamine/Zn ratio of 10 would be a pure aminolysis reaction resulting in the formation of ZnO nanocones. On the other hand, keeping the same amine-to-Zn ratio while using a higher reaction temperature of 210 °C would result in a mixed thermal decomposition and aminolysis reaction, together with an increased reaction rate due to the increased temperature. Thus, the reaction at 210 °C resulted in the formation of ZnO nanobullets where the top cone shape of the nanobullets was explained by the capping effect of the excess benzylamine. This underlines the dual role of the amine reagent, where on the one hand it is a reagent for the aminolysis reaction, and on the other hand, any excess not involved in the aminolysis reaction acts as a capping agent for the polar ZnO facets. This is further proved by decreasing the benzylamine/Zn ratio to 1 while keeping the reaction temperature at 210 °C, resulting in the formation of nanorods without the cone-shaped tip due to the absence of excess benzylamine, which would take the function of a capping agent. An increase of the ratio to 40 resulted in nanoplate formation due to the strong coordination of excess benzylamine to the polar Zn^{2+} surface, inhibiting growth along the [001] direction. It has to be mentioned that the heating rate was also found to have a pronounced effect on the resultant morphology in this system, where rapid heating resulted in the ZnO nanoplates, while slow heating (~ 5 °C/min) to the same reaction temperature led to the formation of "uncompleted" ZnO nanocones (Chang and Waclawik, 2012).

While oleylamine has been widely used as a surfactant and morphology-controlling agent in the synthesis of ZnO nanostructures, oleic acid would be another possible interesting surfactant for morphology control due to its strong coordination ability with the ZnO surface. Usually, however, OA was used in combination with amines (Choi S.H. et al., 2005; Yin et al., 2004) during the synthesis of ZnO, which makes it hard to determine the role of each in the formation of the anisotropic structure. Zhong et al. used a mixture of OA and oleyl alcohol to synthesize ZnO nanostructures from zinc acetate by the well-known ester elimination reaction. In this system, the alcohol acts as a solvent and reagent for the formation of ZnO from zinc acetate through an "esterification alcoholysis reaction", while the OA acts as a surfactant and structure-directing agent. By adjusting the relative amount of oleic acid to oleyl alcohol, while keeping the total volume of the mixture constant, it was possible to obtain a range of complex nanostructures such as spiked ZnO nanostructures (**Fig. 8(a)**) and ZnO tetrapods of various dimensions (**Fig. 8(b)** and **(c)**). By increasing the relative amount of oleyl alcohol and decreasing the relative amount of oleic acid, smaller-sized ZnO tetrapods were obtained due to the increased reaction rate of the alcohol with the precursor, which results in a large number of initial nuclei in a short time (Zhong et al., 2007). Similarly, Zhang et al. also obtained Mn-doped ZnO tetrapods and multipods from bulk ZnO using OA and oleyl alcohol in the non-coordinating solvent 1-octadecene (Zhang and Li, 2009). The use of other alcohols like 1,12-dodecanediol and 1-hexadecanol with oleic acid and zinc acetate yielded ZnO nanocones (Joo et al., 2005a) and nanotriangles (Andelman et al., 2005), respectively.

Oleic acid was also used as a capping agent without any other additives in the non-polar solvent *n*-octadecene. In this medium, previously prepared zinc oleate was used as a precursor with further addition of oleic acid as the surfactant, and the mixture reacted under reflux. Interestingly, defined triangular and hexagonal two-dimensional plate-like structures were formed with prolonged reflux time (**Fig. 9(a)**). The formation of these two-dimensional thin plate-like ZnO structures of about 10 nm in thickness is attributed to the strong binding affinity of oleic acid to the chemically active Zn^{2+} terminated (0001) surface, which prevents further growth in this direction (*c*-direction) (Chiu et al., 2008). While a longer synthesis time yielded more defined shapes, it was also observed that a thinning of the central area of the ZnO platelets took place (**Fig. 9(b)**), which was correlated to an etching activity of the bound

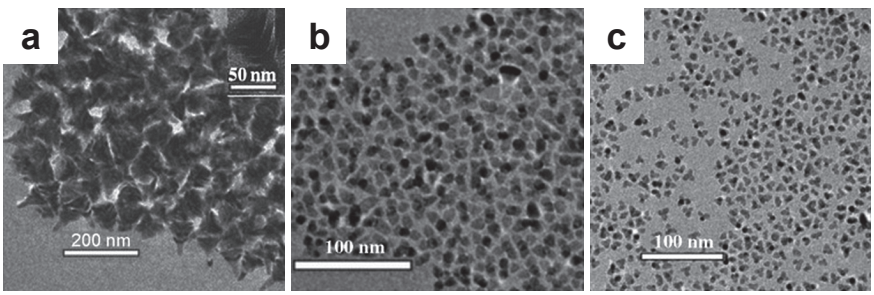

Fig. 8 TEM images of **(a)** ZnO spiked clusters formed using a volume ratio of 1:2 oleic acid to oleyl alcohol, **(b)** large ZnO tetrapods formed using a volume ratio of 1:3.5 oleic acid to oleyl alcohol and **(c)** small ZnO tetrapods formed using a volume ratio of 1:8 oleic acid to oleylamine while keeping the total volume constant. Adapted with permission from Ref. (Zhong et al., 2007). Copyright 2007 Wiley-VCH.

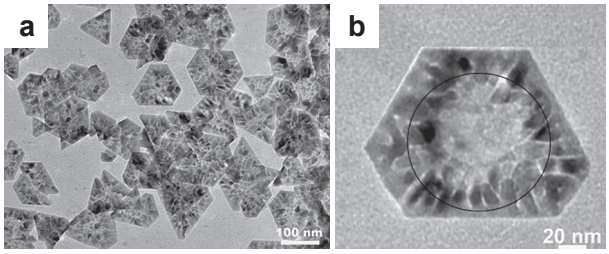

Fig. 9 TEM images of two-dimensional ZnO platelets **(a)** showing the different triangular and hexagonal platelet structures formed after 90 min synthesis time and **(b)** an individual ZnO platelet formed after 120 min synthesis time showing a thinning effect in the center with increased synthesis time. Adapted with permission from Ref. (Chiu et al., 2008). Copyright 2008 Elsevier.

oleic acid. Thus, it was predicted that even longer reflux times could yield ring-like ZnO structures (Chiu et al., 2008).

The use of ethylene diamine as a short-chain diamine was reported to yield micrometer-long ZnO nanorods in alcohols (Panchakarla et al., 2007). Hexamethylenetetramine (HMTA) was also used as a surfactant for the synthesis of ZnO nanorods from $Zn(acac)_2$ in the coordinating solvent trioctylamine at a low temperature, where an increase in the surfactant-to-precursor ratio resulted in well-defined nanorods with a higher aspect ratio. However, increasing the reaction temperature from 70 °C to 140 °C while maintaining the HMTA to $Zn(acac)_2$ constant resulted in a decrease in the aspect ratio, forming less anisotropic structures (Devarepally et al., 2012). Alternatively, polyvinylpyrrolidone (PVP) in ethanol was reported to result in nanorods at a low temperature (80 °C) with good crystallinity (Wang et al., 2005), showing that strongly coordinating ligands such as amines are not necessary for nanorod growth.

The formation of ZnO from zinc acetate and a hydroxide is a typical precipitation reaction that can also be performed in organic media, and as no water was added to the system, this can still be interpreted as a non-aqueous synthesis. Alcohols like methanol and ethanol have been mainly used as solvents, where usually an alcoholic solution of NaOH or KOH is added to a zinc salt dissolved in the same alcohol. While ZnO nanorods have been mainly obtained at higher temperatures (Cheng and Samulski, 2004; Pacholski et al., 2002; Rai et al., 2013), interwoven ZnO nanosheets were obtained when the reaction was performed at room temperature (Khokhra et al., 2015) which shows that the reaction temperature is also a crucial factor for tuning the shape of the nanostructures obtained.

3.3 Effect of precursor type

The type of metal oxide precursor used also has a significant influence on the nanostructure obtained. Heating different zinc alkylcarboxylate precursors in TOP using

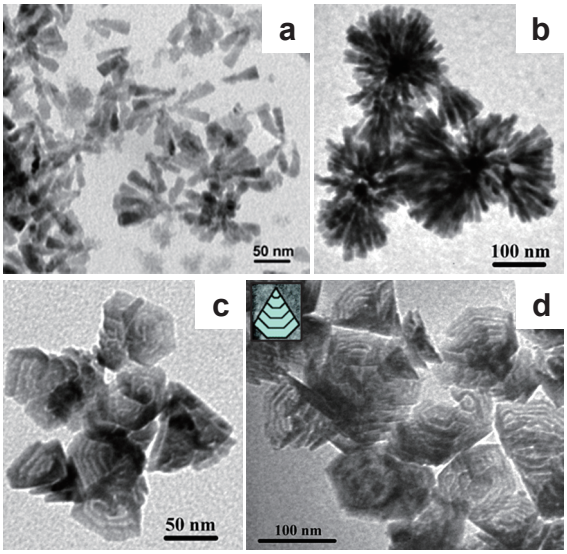

Fig. 10 TEM micrographs of ZnO nanostructures formed from different zinc carboxylate precursors: **(a, b)** multiarmed ZnO nanostructures formed of nanotetrahedrons obtained from **(a)** zinc acetate and **(b)** zinc hexanoate, **(c, d)** squamous ZnO nanostructures produced from **(c)** zinc octanoate and **(d)** zinc oleate. The inset of **(d)** shows a schematic of the structure of the squamous nanocrystals. Adapted with permission from Ref. (Zhang Z. et al., 2006). Copyright 2006 American Chemical Society.

oleylamine as a surfactant results in various types of nanostructures. Zinc salts of short alkyl chain carboxylic acids, such as zinc acetate and zinc hexanoate, resulted in the formation of multiarmed ZnO nanostructures formed of nanotetrahedrons, while precursors containing longer-chain carboxylates like zinc octanoate and zinc oleate produced "squama-like" (fish scale-like) nanostructures (**Fig. 10**) (Zhang Z. et al., 2006). In these non-aqueous synthesis methods, the oleylamine attacks the carboxylates in an aminolytic reaction resulting in amide elimination and ZnO formation. The change in morphology with precursor type was attributed to the difference in the reactivity of the precursor to the oleylamine, thus modulating the rate of the aminolytic reaction. With an increasing chain length of the carboxylate in the precursor, the steric hindrance increased, resulting in a decrease of the aminolysis rate at the coordinated {110} planes but leaving the growth in the [001] direction unhindered. Thus, precursors containing shorter-chain carboxylates formed nanotetrahedrons, while the longer-chain carboxylate precursors formed squamous-like nanocrystals, where the strong binding affinity and steric effects of the longer-chain carboxylates such as oleate to the (110) plane leads to further suppression of the growth in the [110] direction, forming very thin "nanosquamas" (Zhang Z. et al., 2006).

In a separate study by Xu et al., different precursors also resulted in a good variation of particle morphology when used in tetrahydrofuran (THF). While zinc acetate resulted in hexagonal-based pyramidal particles, using $Zn(acac)_2$

instead led to isotropic particles arranged in a cauliflower-like morphology (Xu et al., 2009). The decomposition temperature of each precursor in the same solvents already gives a clue about the different behavior of different precursors. Kunjara Na Ayudha et al. found that the solvothermal synthesis of ZnO from zinc acetate in the non-polar solvents decane and toluene was not feasible at 250 °C, and the synthesis temperature needed to be increased to 300 °C to obtain ZnO nanorods (Kunjara Na Ayudhya et al., 2006). On the other hand, it was possible to obtain ZnO from $Zn(acac)_2$ in decane and toluene at the much lower temperature of 120 °C. In that case, completely different morphologies were obtained where the synthesis in decane resulted in truncated hexagonal pyramidal particles, while in toluene hourglass-like particles were obtained (Xu et al., 2009).

3.4 Effect of precursor concentration

It is generally known from different reaction systems that nanocrystal growth is highly dependent on the monomer concentration. A low monomer concentration usually results in isotropic growth while a high monomer concentration results in an anisotropic growth profile due to the different growth rates of the diverse crystal facets (Manna et al., 2000; Peng and Peng, 2002). In the synthesis of ZnO nanoparticles in a basic methanolic solution of zinc acetate dihydrate, it was observed that by simply increasing the Zn precursor concentration (10-fold compared to the concentration yielding spherical particles), anisotropic ZnO nanorods could be obtained (Pacholski et al., 2002). Similar observations were also made for the microwave-assisted synthesis of ZnO from zinc acetylacetonate in 1-butanol, where an increase of the precursor concentration increased the aspect ratio of the formed nanoparticles, resulting in ZnO nanorods (Ambrožič et al., 2011).

While in some systems, no effect of the precursor concentration on the resulting morphology of the nanoparticles was detected—although an increase of the overall particle size was still observed (Ambrožič et al., 2010; Tonto et al., 2008)—the influence of precursor concentration was more pronounced in other systems (Ambrožič et al., 2011; Pacholski et al., 2002), which underlines the fact that it is an interplay of the precursor type used and overall synthesis conditions used. In this context, Ambrožič et al. observed a concentration-dependent morphology change when using microwave irradiation, whilst a concentration-independent behavior was observed for the same reaction system using reflux conditions with conventional heating (Ambrožič et al., 2010; 2011).

3.5 Effect of doping

It was also observed that doping could affect the anisotropic growth of metal oxide nanoparticles. Co- and Mn-doping of ZnO nanorods synthesized in benzyl alcohol was found to decrease the aspect ratio of the resulting ZnO nanorods, with the effect of Co-doping on the nanorod aspect ratio being more pronounced (Djerdj et al., 2008b).

3.6 Other factors

There are different non-trivial factors that can significantly affect the growth behavior of nanocrystals in the reaction system studied but they are usually overlooked. While the effects of solvents, ligands or surfactants, types of metal oxide precursors, solvent/surfactant/precursor ratios, reaction temperature and synthesis time are the most-studied factors, some other factors can still significantly affect anisotropic crystal growth. Zhao et al. investigated the influence of the mixing time of the precursor, dicyclohexyl zinc, with the ligand, dodecylamine, on the anisotropic growth of ZnO particles (Zhao et al., 2021). A mixing time of more than 6 hours before the start of the actual hydrolysis reaction was found to inhibit the anisotropic particle growth, which was ascribed to the increasing viscosity of the reaction mixture with increasing mixing time, subsequently hindering the anisotropic growth of ZnO through the oriented attachment mechanism (Zhao et al., 2021). Thus, whilst many different factors have been identified that facilitate the synthesis of ZnO nanostructures with anisotropic morphologies, a particular reaction system must always be understood in detail to enable proper control of the particle properties.

4. Iron oxide

Iron oxide is one of the most important magnetic materials, and iron oxide nanocrystals with defined properties are used in manifold applications such as magnetic storage media and magnetic resonance imaging (MRI) (Ajinkya et al., 2020; Teja and Koh, 2009). Anisotropy can be used to modulate the magnetic properties of such nanoparticles where it was found that anisotropic iron oxide nanoparticles possess improved magnetic properties (Zhang et al., 2009). Tuning the shape of the iron oxide nanoparticles results in the exposure of different crystal facets that could be used to vary the T_1 and T_2 proton relaxation time shortening effects, which in turn is important for the design of efficient MRI contrast agents (Zhou et al., 2015). **Table S3** in the supplementary material summarizes the state of the literature on the synthesis of anisotropic iron oxide nanocrystals in non-aqueous media in chronological order.

Whilst typically, magnetite (Fe_3O_4) is the desired material, maghemite (γ-Fe_2O_3) shows similar ferromagnetic behavior and is obtained under more oxidative conditions. As magnetite particles may oxidize during extended storage, particularly in aqueous media, the direct synthesis of maghemite might thus provide a more stable product (Grabs et al., 2012; Masthoff et al., 2014). In non-aqueous reaction systems for the synthesis of iron oxide, surfactants are typically required to obtain particle shapes other than

spheres. The use of long-chain amines such as dodecylamine was found to result in the formation of large hexagon-shaped γ-Fe_2O_3 particles from iron pentacarbonyl ($Fe(CO)_5$) at a surfactant-to-precursor ratio of at least 10. Lower ratios resulted in a mixture of spherical, triangular and diamond-shaped nanocrystals (Cheon et al., 2004). Unique star-shaped Fe_3O_4 nanocrystals were obtained by the use of the bulky 1-adamantanecarboxylic acid instead of the linear oleic acid as the surfactant together with oleylamine (**Fig. 11**) (Zhang L. et al., 2006). It was proposed that the growth mechanism resulting in the anisotropic star shape is based on the bulkiness of the 1-adamantanecarboxylic acid surfactant molecules. Due to their bulkiness, some sites were not covered by the surfactant molecules and led to their further growth, which resulted in the observed spikes of the star-shaped nanocrystals. Further substitution of oleylamine with the bulky 1-adamantaneamine so that the surfactant system is composed of 1-adamantanecarboxylic acid and 1-adamantaneamine instead of the traditional oleic acid/oleylamine surfactant system resulted in a certain anisotropy where irregular-shaped particles were obtained forming flower-like aggregates (Zhang L. et al., 2006). With a ternary surfactant mixture of oleic acid, oleylamine and hexadecane-1,2-diol in a ratio of 3:3:5, it was even possible to produce tetrapod-shaped maghemite nanocrystals from $Fe(CO)_5$ (**Fig. 12**) (Cozzoli et al., 2006). Increasing the precursor concentration of resulted in an increase in anisotropic growth that led to longer tetrapod arms. It was also found that a significant deviation from the optimized 3:3:5 ratio of the three-component surfactant system—or omitting any of these surfactants from the reaction system—resulted in a loss of the tetrapod geometry, which shows the important role of all surfactants in this specified ratio in forming the unique tetrapod geometry (Cozzoli et al., 2006). Analogous tripods, or shamrock-shaped particles, of nickel manganese ferrite were interestingly obtained in a much more facile synthesis without surfactants via an oriented attachment mechanism (Masthoff et al., 2015). Hofmann et al. also investigated the influence of the surfactant ratio of the surfactant system of trioctylamine and oleic acid on the morphology of iron oxide nanoparticles and found that the nanocrystal shape is significantly influenced by the surfactant ratio used. Increasing the trioctylamine to oleic acid ratio resulted in the formation of cubic wüstite iron oxide nanocrystals with concave faces which were referred to as nanotetracubes (Hofmann et al., 2008).

Fatty acid surfactants such as oleic acid were used in several studies, often in the form of its oleate anion as part of the iron oxide precursor. Typically, iron(III) oleate is first synthesized in a separate step and the purified precursor is then mixed with the solvent and heated for the actual synthesis. In this case the oleate already present in the precursor can act as a surfactant and structure-directing agent. Heating the iron oleate complex in 1-octadencene at 320 °C for one hour resulted in cubic iron oxide nanocrystals (Kwon et al., 2007). In another study, the controlled decomposition of the iron oleate precursor at a low temperature of 150 °C in the same solvent formed iron oxide nanowhiskers. At temperatures higher than 300 °C, spherical particles were formed, as commonly reported in the literature. Thermogravimetric analysis (TGA) and density functional theory (DFT) calculations revealed the dissociation of two of the three oleate ligands from the complex at 150 °C, and the third bound oleate ligand was assumed to act as a structure-directing agent for the formation of the one-dimensional nanowhiskers (Palchoudhury et al., 2011a). The addition of the weakly binding surfactant TOPO to a system of iron oleate and oleic acid at a ratio of 6.3:1 (TOPO/OA) resulted in the formation of iron oxide nanoworms, which was attributed to the controlled aggregation of spherical nanoparticles (Palchoudhury et al., 2011b).

A plethora of different iron oxide nanocrystal shapes were accessed by the use of oleate salts instead of oleic acid as the surfactant. Although the oleate ligands in the

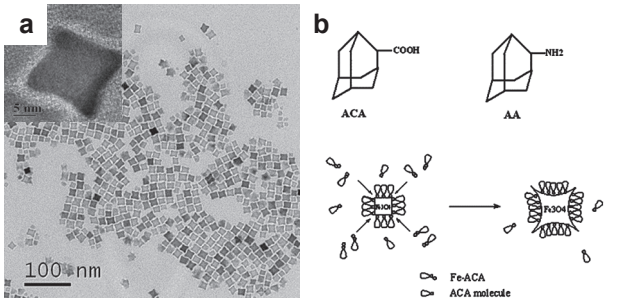

Fig. 11 **(a)** TEM image of iron oxide nanostars obtained using the bulky 1-adamantanecarboxylic acid as a surfactant. The inset shows the HRTEM image of a single iron oxide nanostar. **(b)** Schematic illustration showing the proposed formation mechanism of iron oxide nanostars. Adapted with permission from Ref. (Zhang L. et al., 2006). Copyright 2006 Elsevier.

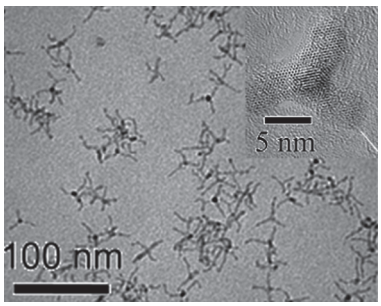

Fig. 12 TEM image of tetrapod maghemite nanocrystals formed through a 3:3:5 surfactant ratio of oleic acid, oleylamine and hexadecane-1,2-diol. The inset shows a HRTEM image of a single tetrapod nanocrystal viewed along the <111> zone axis. Adapted with permission from Ref. (Cozzoli et al., 2006). Copyright 2006 American Chemical Society.

precursor can act as a surfactant, further addition of oleic acid and sodium oleate to the reaction mixture has a significant influence on the shape evolution of the iron oxide nanocrystals. Kovalenko et al. observed that replacing the surfactant oleic acid with its sodium or potassium salt in a reaction system containing iron oleate as a precursor results in the formation of cubic instead of spherical iron oxide nanocrystals. Decreasing the sodium oleate-to-iron oleate precursor ratio even resulted in bipyramidal nanocrystals. From conductivity measurements, it was inferred that the oleate salts in octadecene dissociate at temperatures above 220–230 °C, resulting in ionic oleate species, which is not the case for oleic acid; this difference was related to the different shape evolution (Kovalenko et al., 2007). Similarly, Bao et al. synthesized iron oxide nanorods from iron oleate in benzyl ether by replacing oleic acid with sodium oleate as surfactant, whereby the aspect ratio of the product could be carefully tuned by varying the synthesis temperature (Bao et al., 2012).

A broad range of different iron oxide nanocrystal shapes was also synthesized by Gao's group through variation of the sodium oleate-to-iron oleate molar ratio and using 1-octadecene or trioctylamine as a solvent (**Fig. 13**) (Zhou et al., 2015). Increasing this ratio in 1-octadecene resulted in an increased exposure of the {111} facets, which led to the shape evolving from spherical particles (in the absence of sodium oleate) to hexagonal plates, truncated octahedrons, and finally to tetrahedrons (**Fig. 13(b)–(d)**). Accordingly, it was assumed that the oleate ions preferentially attached to the {111} facets, thus stabilizing them and retarding their growth, which resulted in an increased exposure of the {111} facets with an increasing sodium oleate amount. Using trioctylamine as the solvent, in which higher synthesis temperatures are possible, iron oxide nanocubes (**Fig. 13(e)**) were obtained at low sodium oleate-to-iron oleate ratios (NaOL/FeOL ≤ 1:10), while at a ratio of 2:10, spikes started to emerge at the cube corners forming what the authors called "concave" nanocrystals (**Fig. 13(f)**). A further increase of the sodium oleate amount (NaOL/FeOL = 5:10) resulted in assembled nanostructures which were supposedly formed through the oriented attachment of smaller building blocks (**Fig. 13(g)**). Using low NaOL to FeOL ratios (NaOL/FeOL = 1:10) that previously resulted in nanocubes formed multibranched iron oxide nanoparticles when higher dilutions were used (i.e. lower concentrations of NaOL and FeOL in the system) (**Fig. 13(h)**) (Zhou et al., 2015).

In addition, the use of long-chain quaternary ammonium salts such as tetraoctylammonium bromide was found to induce anisotropic iron oxide nanocrystal growth where nanooctahedra were obtained from the iron oleate precursor. In this system, the authors also addressed the fact that chemical species formed in situ during the synthesis can play an important role in determining the shape of the synthesized nanoparticles (Shavel et al., 2009).

Besides the amount of surfactant or the surfactant-to-precursor ratio, some other non-trivial factors were described to influence the anisotropic growth during the non-aqueous and non-hydrolytic synthesis. Recently, the effect of nitrogen purging on the anisotropic growth of iron oxide nanoparticles was investigated by AbuTalib et al. (2021). Through testing different configurations for nitrogen flow, it was found that bubbling the reaction mixture with nitrogen induced anisotropic growth in their system, while applying nitrogen flow over the reaction mixture reduced the anisotropic growth, and finally the use of only a

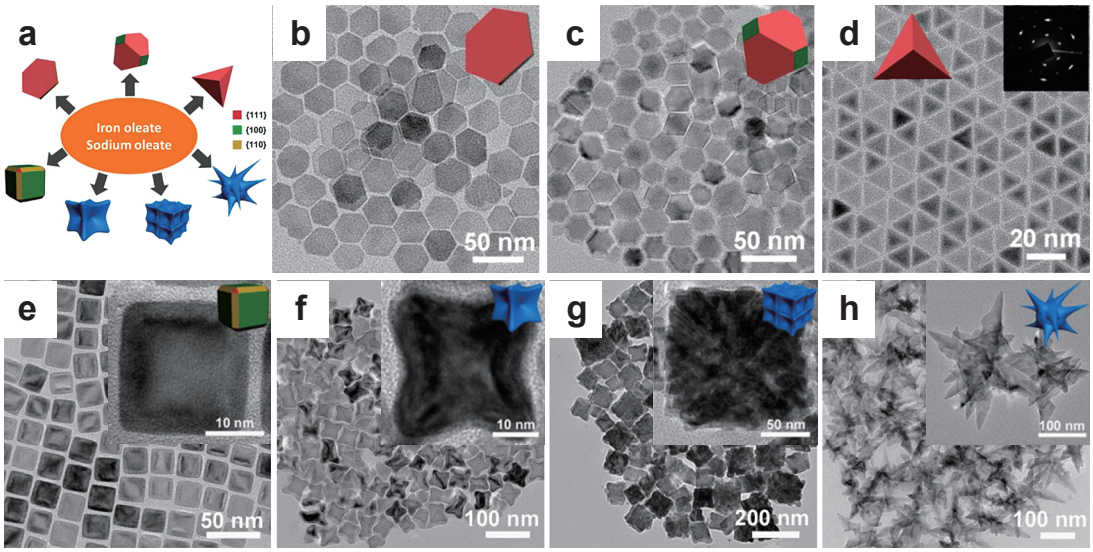

Fig. 13 **(a)** Overview of the different iron oxide particle morphologies obtained using iron oleate as a precursor and sodium oleate as a surfactant; TEM images showing iron oxide **(b)** nanoplates, **(c)** truncated octahedrons, **(d)** tetrahedrons obtained in 1-octadecene and **(e)** nanocubes, **(f)** concave particles, **(g)** assembled structures and **(h)** multibranched nanocrystals obtained in trioctylamine using different sodium oleate-to-iron oleate ratios. Adapted with permission from Ref. (Zhou et al., 2015). Copyright 2015 American Chemical Society.

"nitrogen blanket" (i.e. positive pressure of nitrogen in the system without steady flow) favored isotropic crystal growth. The nitrogen flow rate did not play a significant role in the extent of anisotropic growth. It is assumed that the reason for this anisotropy observed in the nitrogen-bubbling system arises from increased turbulence, the bubbles acting as nucleation sites and inducing aggregation, or the improved removal of volatile by-products from the system which otherwise influence the particle morphology (AbuTalib et al., 2021). Additionally, a significant influence of the amount of the oleylamine surfactant relative to the $Fe(acac)_3$ precursor on the morphology of the product was found in this system. While at very high oleylamine-to-precursor ratios (above 40 equivalents), isotropic particles were observed, decreasing the oleylamine amount to 25 equivalents resulted in anisotropic nuclei which formed iron oxide nanocrystals with two branches (bipods). A further decrease in the oleylamine amount to 17 equivalents resulted in multiply branched nanocrystals and finally branched nanocrystals with a flower-like appearance at 15 equivalents of oleylamine. An investigation of the evolution of the branched iron oxide nanocrystals over time revealed the formation of small anisotropic nuclei in most cases, which further aggregate in the initial stages of the synthesis forming polycrystalline nanocrystals. The defects and misalignments in the formed aggregates are then removed through rearrangement and ordering over the course of the reaction, and finally monocrystalline branched iron oxide nanocrystals are obtained.

Prolongation of the synthesis time also has an influence on the product morphology. While the decomposition of iron oleate in 1-octadecane at 320 °C results in the formation of monodisperse spherical nanocrystals for a synthesis time up to 30 minutes (Park et al., 2004a), an increase of the synthesis time to one hour resulted in monodisperse cubic nanocrystals (Kwon et al., 2007). The spherical iron oxide nanocrystals are converted to cubic nanocrystals upon prolonged aging at 320 °C, forming the thermodynamically most stable shape for the iron oxide spinel structure with only {100} planes exposed (Kwon et al., 2007). A change of shape with reaction time was also observed during the synthesis of iron oxide from iron(II) acetate in trioctylamine using oleic acid as the surfactant at 255 °C. While at shorter synthesis times (10–25 min) cubic nanocrystals were formed, the particles transformed into truncated octahedrons when the reaction time was prolonged further (Redl et al., 2004).

Two-dimensional iron oxide nanocrystals obtained from non-aqueous and non-hydrolytic synthesis are still rare and the parameters and conditions required for their synthesis are still not well understood. Examples of such two-dimensional iron oxide nanocrystals were presented by Casula et al., where circular nanodisks were obtained from iron pentacarbonyl in octyl ether using tridecanoic acid as the surfactant (Casula et al., 2006). It is important to note that the disk form of the obtained nanoparticles has been confirmed through AFM height measurements. In general, even if TEM investigations reveal a spherical nanocrystal appearance, it is important to investigate the true height of the nanoparticles to prove their isotropy or anisotropy, but this is usually not performed in most of the published works so far. In another work, hexagonal and triangular iron oxide nanoplates were obtained in diethylene glycol from iron(III) chloride without the use of any surfactant (Zhang et al., 2009).

5. Other metal oxides

A number of other metal oxides and mixed-metal oxides have been synthesized as anisotropic nanocrystals via non-aqueous synthesis routes. As there are only a few reports about each, they are discussed in this section in combined form. **Table S4** in the supplementary material provides an overview of the materials and morphologies obtained and the respective synthesis conditions. In the following paragraphs, some more insight will be given for some of these reaction systems.

Zirconia nanocrystals synthesized in benzyl alcohol using sodium lauryl sulfate as a surfactant showed one-dimensional growth when $ZrOCl_2 \cdot 8H_2O$ was used as the precursor, while $Zr(SO_4)_2 \cdot H_2O$ yielded only isotropic nanoparticles (Siddiqui et al., 2012). The reaction of zirconium *n*-propoxide in benzyl alcohol was reported to lead to fractal nanostructures, in particular at lower reaction temperatures and extended reaction times (Stolzenburg et al., 2016).

The synthesis of V_2O_3 from $VOCl_3$ in benzyl alcohol led to ellipsoidal-shaped nanorods (Niederberger et al., 2002b; Ohayon and Gedanken, 2010), whereby doping with the rare earth metals Gd and Nd resulted in an alteration of the morphology to nanoflakes and nanocubes, respectively (Venkatesan et al., 2015).

Due to the great potential of tungsten oxide in different fields, such as for batteries, gas sensing, as well as photocatalytic and electrochromic applications, different non-aqueous synthesis procedures for tungsten oxide nanorods or nanowires have been developed (Choi H.G. et al., 2005; Lee et al., 2003; Polleux et al., 2006; Woo et al., 2005). Woo et al. conducted a systematic study which revealed that the aspect ratio of tungsten oxide nanorods could be tuned through the coordinating power of the surfactant system used. Increasing the coordinating power was thereby found to decrease the tungsten oxide nanorod length, which was attributed to the increased inhibition of growth in the [010] direction resulting from the stronger ligand binding (Woo et al., 2005). In a different approach, Choi et al. were able to tune the aspect ratio of tungsten oxide nanorods by adjusting the precursor concentration in an ethanolic solution, without the need for any surfactant.

Using lower WCl_6 precursor concentrations resulted in higher aspect ratios and even in the growth of tungsten oxide nanowires (Choi H.G. et al., 2005). To obtain more complex structures, Zhao et al. added urea to the ethanolic WCl_5 precursor solution to act as a ligand and structure-directing agent due to its strong hydrogen bonding ability. This enabled the formation of tungsten oxide nanotubes using a template-free non-aqueous synthesis for the first time, whereby the as-synthesized product was identified as tungstic acid hydrate ($H_2W_{1.5}O_{5.5}\cdot H_2O$) and was transformed to WO_3 through calcination without loss of the hollow structure (Zhao and Miyauchi, 2008). Variation of the synthesis parameters, such as the urea amount and reaction time, yielded further hollow tungstic acid hydrate nanostructures (hollow spheres and boxes), which were converted to tungsten trioxide upon calcination. Interestingly, a broad range of morphologies was obtained thereby, which was attributed to different self-assembly processes of smaller nanoparticles and nanorods due to the presence of urea in the reaction system (Zhao and Miyauchi, 2009).

There has also been an interest in synthesizing manganese oxide due to its magnetic properties, especially at the nanoscale (Park et al., 2004b). Uniform MnO nanorods were obtained by Park et al. through injecting a previously prepared manganese oleylamine complex into trioctylphosphine or triphenylphosphine at high temperatures (330 °C) (Park et al., 2004b). Zitoun et al. were able to prepare MnO multipods via the decomposition of $Mn(oleate)_2$ in *n*-trioctylamine in the presence of oleic acid at 320 °C, where the arms showed an arrow-like ending and a zigzag structure which indicated an oriented attachment process of the initially formed cube-shaped or truncated octahedral nuclei (Zitoun et al., 2005). Similar anisotropic MnO nanoparticle shapes termed as "dumbbell-shaped" MnO nanocrystals were obtained by Zhong et al. through the use of manganese formate hydrate as a precursor (Zhong et al., 2006). Anisotropic shapes for manganese cobalt oxide ($MnCoO_x$) ternary mixed-metal oxides were obtained through the decomposition of $Mn(oleate)_2$ and $Co(oleate)_2$ precursors in 1-octadecene in the presence of oleic acid (Gliech et al., 2020). Interestingly, the use of a single metal oxide precursor in this system yielded cubic or octahedral shapes for manganese oxide and aggregated octahedral shapes for cobalt oxide, while for the mixed-metal oxide, rod-, T-, cross- and hexapod-shaped nanocrystals were obtained with decreasing cobalt concentrations. A new solution-solid-solid (SSS) oxide mechanism was suggested for the anisotropic growth of the mixed-metal oxide nanoparticles, which is a good example of the influence of other metal ions on the anisotropic growth of metal oxides. In the suggested SSS growth mechanism, first MnO nuclei are formed, followed by the deposition of Co monomers to form Co-rich regions which serve as sites for outward growth in the <100> directions, thus forming the arms. At low Co concentration, the Co has time to accumulate on different facets of the MnO nuclei, thus forming several starting points for the branching, resulting in multiarmed structures such as hexapods. Increasing the Co concentration decreases the cobalt accumulation time and less branched structures occur, thus leading to nanorod structures at high concentrations (Gliech et al., 2020).

Even more exotic metal oxides such as actinide oxides have been synthesized using the non-aqueous and non-hydrolytic synthesis route. In several cases, the use of certain surfactants and certain synthesis conditions yielded anisotropic shapes for those oxides. For example, anisotropic thorium oxide (ThO_2) has been obtained from thorium acetylacetonate in benzyl ether using a ternary surfactant mixture of TOPO, OA and trioctylamine at 280 °C (Hudry et al., 2012).

6. Oriented attachment mechanisms resulting in anisotropic structures

Different mechanisms have been reported to potentially lead to the formation of anisotropic nanoparticles or nanostructures such as controlled aggregation (for example via oriented attachment), etching and branching (AbuTalib et al., 2021). According to the classical crystallization model, anisotropic growth in metal oxides can be mainly achieved via kinetic control through the use of surfactants or by the selective formation of nuclei of specific crystal phases featuring different surface energies (Jun et al., 2006; Sajanlal et al., 2011). Besides the classical crystallization theory, oriented attachment has been proven to represent an important pathway to result in anisotropic metal oxide nanocrystals.

The oriented attachment mechanism is based on the controlled aggregation of nanoparticle building blocks showing an aligned crystal orientation towards each other and thus, in principle, leads to one larger crystal. Thereby, isotropic metal oxide nanoparticles can also be used as building blocks for larger anisotropic and more complex three-dimensional structures. This process can be observed in the absence of organic surfactants which delimits this process from usual self-assembly phenomena that occur due to organic building blocks. This phenomenon was identified to represent an important non-classical crystal growth mechanism and was found in many systems including non-aqueous and/or non-hydrolytic metal oxide synthesis (Chen et al., 2022; Pacholski et al., 2002; Xue et al., 2014). Kinetic models describing the oriented attachment process have been developed by Ribeiro et al. (2005; 2006).

The general mechanism for the formation of anisotropic nanoparticles or nanostructures from smaller (usually isotropic) nanoparticles was identified to consist of the following steps: 1) Collisions of nanoparticles leading to their loose attachment where sometimes the crystal planes are

already aligned, 2) Rotation of the attached nanoparticles takes place to eliminate some misorientation, 3) Smoothening of the surface occurs due to further monomer addition and eventually Ostwald ripening (**Fig. 14**) (Lee et al., 2005; Xue et al., 2014). Interestingly, this process can occur in some systems even at room temperature without the addition of specific ligands (Leite et al., 2003), while higher temperatures usually enhance the particle coalescence and thus the oriented attachment process (Lee et al., 2005). The presence of some crystal defects or misalignments such as twinning, stacking faults or dislocations in the final product can give a hint on the crystal evolution through the oriented attachment mechanism (Chen et al., 2022). The oriented attachment process can even give rise to anisotropic growth directions that are generally not accessible through traditional monomer deposition or classical crystal growth (Lee et al., 2005; Leite et al., 2003). The use of selective surfactants can facilitate and direct the oriented attachment process and inhibit Ostwald ripening (Xue et al., 2014). This makes the oriented attachment process a very effective mechanism for achieving novel and even more complex anisotropic structures.

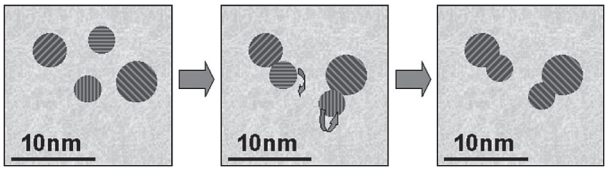

Fig. 14 Schematic showing the collision, attachment and rotation steps involved in the oriented attachment process. Adapted with permission from Ref. (Leite et al., 2003). Copyright 2003 American Institute of Physics.

A good example showing the formation of anisotropic zinc oxide nanorods from quasi-spherical ZnO nanoparticles via oriented attachment in non-aqueous systems was presented by Pacholski et al. (2002). Thereby, a sol of the ZnO nanoparticles previously prepared from a dilute basic methanolic solution of zinc acetate dihydrate (**Fig. 15(a)**) was first concentrated through solvent evaporation. Refluxing of the resulting sol resulted in ZnO nanorods where the dimensions of the nanorods increased with increasing reflux time, yielding excellent monocrystalline ZnO nanorods after one day (**Fig. 15(b)**). Sampling at different time intervals showed the arrangement of the quasi-spherical particles into chains where neck formation and coalescence with excellent alignment of the particle crystal planes was observed in high-resolution TEM images (**Fig. 15(c)–(g)**) (Pacholski et al., 2002). Similar observations were made by Peukert et al. through an in-depth investigation of ZnO nanorod formation kinetics in the same

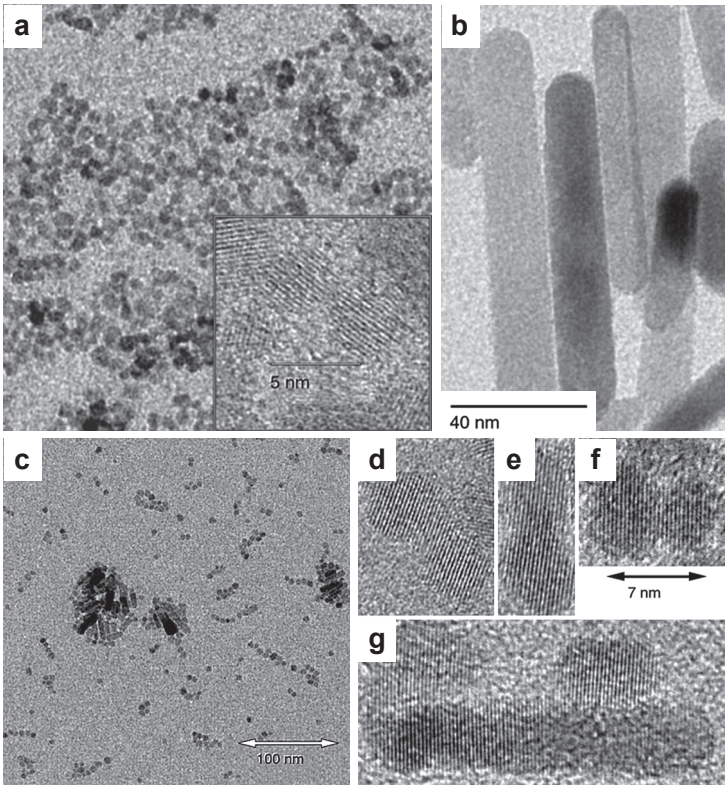

Fig. 15 TEM images of **(a)** quasi-spherical ZnO nanoparticles used as starting sol for the synthesis of ZnO nanorods, **(b)** final monocrystalline ZnO nanorods formed by oriented attachment of the quasi-spherical ZnO particles, **(c)** sample of the reaction mixture after 2 h showing some ZnO nanorods and quasi-spherical ZnO particles arranged in shorter and longer chains, **(d–g)** high-resolution TEM micrographs of differently attached particles showing neck formation and coalescence with aligned crystal planes. Adapted with permission from Ref. (Pacholski et al., 2002). Copyright 2002 Wiley-VCH.

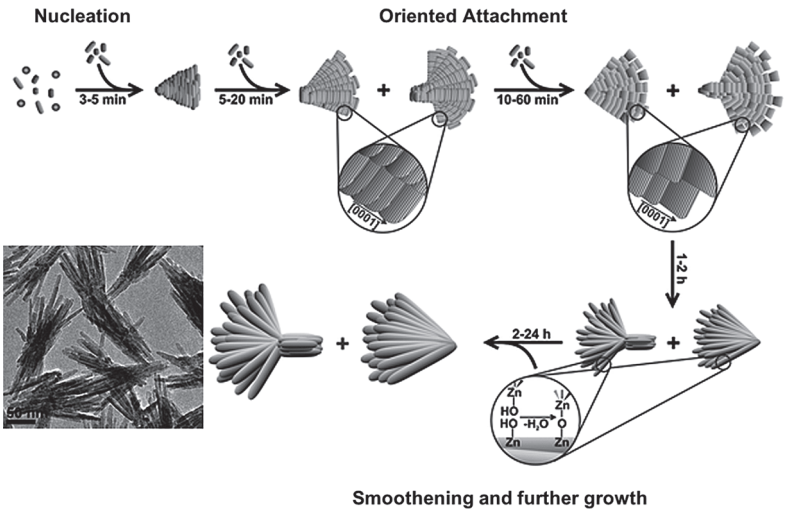

Fig. 16 Schematic showing the steps involved in the temporal evolution of ZnO fan- and bouquet-like nanostructures in benzyl alcohol. Adapted with permission from Ref. (Ludi et al., 2012). Copyright 2012 The Royal Society of Chemistry.

system (Voigt et al., 2010). Buha et al. observed the formation of hexagonal ZnO nanoplatelets from $Zn(acac)_2$ in acetonitrile, which was identified in high-resolution TEM to be a mesocrystal formed of perfectly aligned crystal domains, so that the final hexagonal nanocrystal behaves as a single crystal (Buha et al., 2007). Similarly, the formation of hexagonal Al-doped ZnO (AZO) in benzylamine was observed and investigated via small-angle X-ray scattering (SAXS), where time-resolved analysis revealed oriented aggregation forming hexagonal mesocrystals (Ungerer et al., 2019; 2020). Oriented attachment was also observed for the formation of TiO_2 nanorods when the reaction system of Joo et al. (2005b) (synthesis of TiO_2 from TIP using oleic acid as a surfactant, **Table S1**) was reinvestigated by Dalmaschio and Leite, where even the detachment of well-faceted nanoparticles was observed for longer reaction times and this was interpreted as Rayleigh instability of the TiO_2 originally formed through oriented attachment (Dalmaschio and Leite, 2012). Although Joo et al. (2005b) already observed the presence of spherical nanoparticles along with the synthesized TiO_2 nanorods, the reason behind their presence in the product was not further investigated.

Oriented attachment can also be the reason for the formation of ordered aggregates as was observed in the formation of ZnO nanorod bundles (Zhang et al., 2007). More complex geometries could even be obtained due to oriented-attachment mechanisms such as hollow hexagonal ZnO mesocrystals which form via the oriented attachment of trapezoidal ZnO nanosheets (Wang et al., 2013), interwoven ZnO nanosheets (Khokhra et al., 2015) and fan- and bouquet-like ZnO nanostructures (Ludi et al., 2012). Khokhra et al. proposed that the aggregation of ZnO nanosheets to form an interwoven structure was induced by the interaction of the solvent used with the adsorbed hydroxide and acetate ions on the surface of the ZnO nanocrystals via hydrogen bonds (Khokhra et al., 2015). In a detailed study, the temporal evolution of the fan- and bouquet-like ZnO nanostructures was followed from platelet-like ZnO nanoparticles formed in benzyl alcohol (**Fig. 16**). Overlapping stages of classical nucleation, oriented attachment followed by further growth and surface smoothening could be observed in this reaction system (Ludi et al., 2012).

7. Benzyl alcohol route for anisotropic particle growth

The “benzyl alcohol route” has emerged as a unique non-aqueous synthesis route for multiple metal oxides. The advantage of this route lies in the fact that it is mainly a solvent-directed route which makes it possible to synthesize metal oxides and control their morphology through the variation of different experimental parameters without the need of any surfactants. This is achieved via the coordinating ability of benzyl alcohol to the metal oxide surface, however, compared to surfactants, a relatively low amount of surface organics results, rendering a “clean surface” that is accessible for small molecules, which is important for catalytic or sensing applications (Clavel et al., 2007; Pinna and Niederberger, 2008).

Benzyl alcohol can act as a solvent, reducing agent and structure-directing agent for many metal oxides (Pinna et al., 2011; Qamar et al., 2017). The fact that it can also act as a reducing agent was successfully applied to synthesize several non-stoichiometric metal oxide nanoparticles, which is very useful for catalytic applications where these defects can act as catalytic centers (Qamar et al., 2017). The structure-directing properties of benzyl alcohol are revealed in the formation of different anisotropic metal oxides. Qamar et al. synthesized a series of non-stoichiometric

metal oxides (TiO_x, ZnO_x, SnO_x, CeO_x, In_2O_x and Ga_2O_x) at a high temperature of 245 °C, where for several metal oxides, a square or rectangular plate-like morphology was obtained (Qamar et al., 2017). ZnO nanorods were successfully synthesized in benzyl alcohol from $Zn(acac)_2$ hydrate without the need of any surfactant (Djerdj et al., 2008b). Moreover, Al-doped ZnO formed with a rod-like shape in benzyl alcohol, in contrast to the synthesis in benzylamine where no elongated growth was observed (Zellmer et al., 2015). Similarly, TiO_2 nanorods were obtained in benzyl alcohol from $TiCl_4$ at a temperature as low as 70 °C (Abazović et al., 2008; 2006). While shorter synthesis times of some hours up to one day yielded spherical anatase TiO_2 nanoparticles (Garnweitner and Grote, 2009; Niederberger et al., 2002a), longer synthesis times of three days resulted in the formation of nanorods (Abazović et al., 2008; Jia et al., 2009). The use of TIP as a precursor together with minor amounts of silanes in the benzyl alcohol route yielded platelet-like TiO_2 particles (Koziej et al., 2009), while the use of OLA as a surfactant even resulted in two-dimensional TiO_2 nanosheets (Wu et al., 2008). Interestingly, the analogous synthesis in benzylamine also results in nanosheets that are evenly stacked, proving the tendency of amines to guide the reaction towards the formation of 2-D structures (Garnweitner et al., 2008).

Zirconia nanocrystals synthesized in benzyl alcohol using sodium lauryl sulfate as a surfactant showed one-dimensional growth when $ZrOCl_2{\cdot}8H_2O$ was used as the precursor while $Zr(SO_4)_2{\cdot}H_2O$ yielded only isotropic nanoparticles (Siddiqui et al., 2012). The reaction of zirconium *n*-propoxide in benzyl alcohol was reported to lead to fractal nanostructures, in particular at lower reaction temperatures and extended reaction times (Stolzenburg et al., 2016).

In several cases, the synthesis of metal oxides via the benzyl alcohol route yielded nanoparticles of narrow size distribution together with a surprising tendency of forming well-defined aggregates, sometimes even with two-dimensional or complex three-dimensional anisotropic morphologies. In situ formed organics were often judged to exert a pronounced effect on the nanoparticle and aggregate morphology formed. An in-depth analysis of the organics present on the particle surface as well as organic by-products in the reaction mixture revealed the in-situ formation of benzoate species that adsorb on the nanocrystal surface and thus act as a capping and structure-directing agent (Pinna et al., 2005; Pucci et al., 2012). In another study, the formation of WO_3 nanowire bundles was attributed to the partial oxidation of benzyl alcohol to benzaldehyde which contributed to the formation of nanowire bundles as an inorganic-organic hybrid nanostructure (Polleux et al., 2005; 2006).

The use of additives other than surfactants could also have a significant effect on the formed nanostructures in the "benzyl alcohol route", giving access to novel shapes. For example, the addition of HCl to $Ti(OBu)_4$ in benzyl alcohol enabled the formation of walnut-like aggregate structures composed of rutile-phase nanorods as building blocks. An increase in the amount of HCl added allowed tuning the size of the nanorods and thus, of the formed aggregate structure. It was proposed that the presence of chloride ions supports the anisotropic growth of rutile TiO_2 through selective adsorption to the (110) plane of rutile TiO_2 suppressing its growth, thus favoring the growth in the [001] direction (Kim et al., 2013). In the synthesis of tungsten oxide from WCl_6 in benzyl alcohol, the formation of tungstite ($WO_3{\cdot}H_2O$) nanoplatelets was observed. Upon the addition of the siderophore deferoxamine mesylate as an additive, a fundamental change in the morphology of the resulting tungsten oxide was observed. Tungsten oxide nanowires were obtained, which were arranged in bundles to form inorganic-organic hybrid superstructures (Polleux et al., 2005).

8. Summary and outlook

In this article, the different non-aqueous and/or non-hydrolytic reaction systems used for the synthesis of simple and complex anisotropic metal oxide nanocrystals and nanostructures were summarized. Many examples for the most common metal oxides, in particular titania, zinc and iron oxide as well as for more specialized systems were summarized, showing that there are many parameters controlling the resultant morphology. Moreover, the common theories resulting in anisotropic crystal growth in these non-aqueous systems were elaborated. While some general mechanisms and concepts have been developed for the anisotropic crystal growth in non-aqueous media, some reaction systems are still found to possess some unique features and mechanisms for anisotropic nanostructure formation, such as unique aggregation behavior, and need to be investigated in detail for each system on its own.

To date, the synthesis of anisotropic metal oxides has still largely focused on low-dimensional nanoparticles, and more complex anisotropic structures remain relatively uncommon and need further investigation of the reaction parameters that can yield such structures in a single step or through multi-step approaches. It should be noted that anisotropic metal oxide nanoparticles or nanostructures can be formed directly through either the "truly" anisotropic growth of a single crystal or via an oriented-attachment or controlled-aggregation process, usually leading to polycrystalline anisotropic structures or mesocrystals with certain misalignments and defects. A deeper understanding of the factors governing the controlled aggregation and oriented attachment of nanoparticles in non-aqueous media would help to engineer more complex anisotropic metal oxide nanostructures formed from smaller isotropic or anisotropic building blocks.

Different parameters have been identified to play an important role in anisotropic growth, where surfactants represent a cornerstone in regulating anisotropic particle growth. However, the solvent can also fulfill this function and additionally act as a structure-directing agent. Moreover, the precursor type and its ratio to the solvent, as well as possibly the surfactant, can influence the growth processes and induce the formation of anisotropic structures. This can be attributed to specific precursor decomposition mechanisms, as well as the presence of certain counter ions or ligands from the precursor in the system. The precursor may also contain water from crystallization which can also influence the nanoparticle formation process in various ways. It has to also be taken into consideration that side products formed during the non-aqueous synthesis can coordinate to the nanoparticle surface, resulting in strong modification of the nanoparticle growth and triggering aggregation, even though they might only be formed in very small amounts. The reaction temperature is another substantial factor that affects nanocrystal nucleation and the subsequent reaction rate, which can result in different crystal growth mechanisms. While most of the studies concentrate on factors such as the surfactant used, surfactant concentration, reaction solvent and metal oxide precursor, attention should also be paid to several uncommon factors which need more in-depth investigation in non-aqueous systems such as the heating rate, cooling rate, mixing of reaction components, rate and order of reagent addition, hot-injection of the precursor, etc.

As presented in this contribution, the synthesis of metal oxides in organic media has been intensively studied in the literature, while the preparation of other metal oxides has been only rarely investigated in non-aqueous media. It is important to note that different metal oxide precursors exhibit different reactivity and reaction kinetics, even in similar reaction media, which makes it important to study the shape evolution of each metal oxide in non-aqueous media separately. There is still a high potential for the development of non-aqueous and non-hydrolytic synthesis routes capable of synthesizing various anisotropic metal oxide nanostructures because of the almost infinite possibilities of combining different organic reaction media, metal oxide precursors and surfactants, as well as varying the corresponding reaction parameters.

Supplementary information

The online version contains supplementary material available at https://doi.org/10.14356/kona.2024014.

Acknowledgments

The authors acknowledge funding by the German Research Foundation (Deutsche Forschungsgemeinschaft, DFG), grants GA 1492/9-2 and NI 414/24-2.

References

Abazović N.D., Čomor M.I., Dramićanin M.D., Jovanović D.J., Ahrenkiel S.P., Nedeljković J.M., Photoluminescence of anatase and rutile TiO_2 particles, Journal of Physical Chemistry B, 110 (2006) 25366–25370. DOI: 10.1021/jp064454f

Abazović N.D., Ruvarac-Bugarčić I.A., Čomor M.I., Bibić N., Ahrenkiel S.P., Nedeljković J.M., Photon energy up-conversion in colloidal TiO_2 nanorods, Optical Materials, 30 (2008) 1139–1144. DOI: 10.1016/j.optmat.2007.05.038

AbuTalib N.H., LaGrow A.P., Besenhard M.O., Bondarchuk O., Sergides A., Famiani S., Ferreira L.P., Cruz M.M., Gavriilidis A., Thanh N.T.K., Shape controlled iron oxide nanoparticles: Inducing branching and controlling particle crystallinity, CrystEngComm, 23 (2021) 550–561. DOI: 10.1039/d0ce01291b

Ahmad M.Z., Chang J., Ahmad M.S., Waclawik E.R., Wlodarski W., Non-aqueous synthesis of hexagonal ZnO nanopyramids: gas sensing properties, Sensors and Actuators B: Chemical, 177 (2013) 286–294. DOI: 10.1016/j.snb.2012.11.013

Ajinkya N., Yu X., Kaithal P., Luo H., Somani P., Ramakrishna S., Magnetic iron oxide nanoparticle (IONP) synthesis to applications: Present and future, Materials, 13 (2020) 4644. DOI: 10.3390/ma13204644

Ambrožič G., Orel Z.C., Žigon M., Microwave-assisted non-aqueous synthesis of ZnO nanoparticles, Materiali in Tehnologije, 45 (2011) 173–177.

Ambrožič G., Škapin S.D., Žigon M., Orel Z.C., The synthesis of zinc oxide nanoparticles from zinc acetylacetonate hydrate and 1-butanol or isobutanol, Journal of Colloid and Interface Science, 346 (2010) 317–323. DOI: 10.1016/j.jcis.2010.03.001

Andelman T., Gong Y., Polking M., Yin M., Kuskovsky I., Neumark G., O'Brien S., Morphological control and photoluminescence of zinc oxide nanocrystals, Journal of Physical Chemistry B, 109 (2005) 14314–14318. DOI: 10.1021/jp050540o

Andrade R.G.D., Veloso S.R.S., Castanheira E.M.S., Shape anisotropic iron oxide-based magnetic nanoparticles: synthesis and biomedical applications, International Journal of Molecular Sciences, 21 (2020) 2455. DOI: 10.3390/ijms21072455

Arafat M.M., Dinan B., Akbar S.A., Haseeb A.S.M.A., Gas sensors based on one dimensional nanostructured metal-oxides: a review, Sensors, 12 (2012) 7207–7258. DOI: 10.3390/s120607207

Bakshi M.S., How surfactants control crystal growth of nanomaterials, Crystal Growth and Design, 16 (2016) 1104–1133. DOI: 10.1021/acs.cgd.5b01465

Bao L., Low W.-L., Jiang J., Ying J.Y., Colloidal synthesis of magnetic nanorods with tunable aspect ratios, Journal of Materials Chemistry, 22 (2012) 7117–7120. DOI: 10.1039/c2jm16401a

Bharat T.C., Shubham, Mondal S., S. Gupta H., Singh P.K., Das A.K., Synthesis of doped zinc oxide nanoparticles: a review, Materials Today: Proceedings, 11 (2019) 767–775. DOI: 10.1016/j.matpr.2019.03.041

Buha J., Djerdj I., Niederberger M., Nonaqueous synthesis of nanocrystalline indium oxide and zinc oxide in the oxygen-free solvent acetonitrile, Crystal Growth and Design, 7 (2007) 113–116. DOI: 10.1021/cg060623+

Buonsanti R., Grillo V., Carlino E., Giannini C., Kipp T., Cingolani R., Cozzoli P.D., Nonhydrolytic synthesis of high-quality anisotropically shaped brookite TiO_2 nanocrystals, Journal of the American Chemical Society, 130 (2008) 11223–11233. DOI: 10.1021/ja803559b

Burrows N.D., Vartanian A.M., Abadeer N.S., Grzincic E.M., Jacob L.M., Lin W., Li J., Dennison J.M., Hinman J.G., Murphy C.J., Anisotropic nanoparticles and anisotropic surface chemistry, Journal of Physical Chemistry Letters, 7 (2016) 632–641. DOI: 10.1021/acs.jpclett.5b02205

Cao T., Li Y., Wang C., Shao C., Liu Y., One-step nonaqueous synthesis of pure phase TiO_2 nanocrystals from $TiCl_4$ in butanol and their photo-

catalytic properties, Journal of Nanomaterials, 2011 (2011) 267415. DOI: 10.1155/2011/267415

Casula M.F., Jun Y., Zaziski D.J., Chan E.M., Corrias A., Alivisatos A.P., The concept of delayed nucleation in nanocrystal growth demonstrated for the case of iron oxide nanodisks, Journal of the American Chemical Society, 128 (2006) 1675–1682. DOI: 10.1021/ja056139x

Chang J., Waclawik E.R., Facet-controlled self-assembly of ZnO nanocrystals by non-hydrolytic aminolysis and their photodegradation activities, CrystEngComm, 14 (2012) 4041–4048. DOI: 10.1039/c2ce25154j

Chang S.M., Doong R.A., Characterization of Zr-doped TiO_2 nanocrystals prepared by a nonhydrolytic sol-gel method at high temperatures, Journal of Physical Chemistry B, 110 (2006) 20808–20814. DOI: 10.1021/jp0626566

Chavali M.S., Nikolova M.P., Metal oxide nanoparticles and their applications in nanotechnology, SN Applied Sciences, 1 (2019) 607. DOI: 10.1007/s42452-019-0592-3

Chen R., Nguyen Q.N., Xia Y., Oriented attachment: a unique mechanism for the colloidal synthesis of metal nanostructures, ChemNanoMat, 8 (2022). DOI: 10.1002/cnma.202100474

Chen S., Manders J.R., Tsang S.-W., So F., Metal oxides for interface engineering in polymer solar cells, Journal of Materials Chemistry, 22 (2012) 24202–24212. DOI: 10.1039/c2jm33838f

Cheng B., Samulski E.T., Hydrothermal synthesis of one-dimensional ZnO nanostructures with different aspect ratios, Chemical Communications, 4 (2004) 986–987. DOI: 10.1039/b316435g

Cheon J., Kang N.-J., Lee S.-M., Lee J.-H., Yoon J.-H., Oh S.J., Shape evolution of single-crystalline iron oxide nanocrystals, Journal of the American Chemical Society, 126 (2004) 1950–1951. DOI: 10.1021/ja038722o

Chiu W.S., Khiew P.S., Isa D., Cloke M., Radiman S., Abd-Shukor R., Abdullah M.H., Huang N.M., Synthesis of two-dimensional ZnO nanopellets by pyrolysis of zinc oleate, Chemical Engineering Journal, 142 (2008) 337–343. DOI: 10.1016/j.cej.2008.04.034

Choi H.G., Jung Y.H., Kim D.K., Solvothermal synthesis of tungsten oxide nanorod/nanowire/nanosheet, Journal of the American Ceramic Society, 88 (2005) 1684–1686. DOI: 10.1111/j.1551-2916.2005.00341.x

Choi S.H., Kim E.G., Park J., An K., Lee N., Kim S.C., Hyeon T., Large-scale synthesis of hexagonal pyramid-shaped ZnO nanocrystals from thermolysis of Zn-oleate complex, Journal of Physical Chemistry B, 109 (2005) 14792–14794. DOI: 10.1021/jp052934l

Clavel G., Willinger M.G., Zitoun D., Pinna N., Solvent dependent shape and magnetic properties of doped ZnO nanostructures, Advanced Functional Materials, 17 (2007) 3159–3169. DOI: 10.1002/adfm.200601142

Cozzoli P.D., Snoeck E., Garcia M.A., Giannini C., Guagliardi A., Cervellino A., Gozzo F., Hernando A., Achterhold K., Ciobanu N., Parak F.G., Cingolani R., Manna L., Colloidal synthesis and characterization of tetrapod-shaped magnetic nanocrystals, Nano Letters, 6 (2006) 1966–1972. DOI: 10.1021/nl061112c

Dalmaschio C.J., Leite E.R., Detachment induced by Rayleigh-instability in metal oxide nanorods: insights from TiO_2, Crystal Growth and Design, 12 (2012) 3668–3674. DOI: 10.1021/cg300473u

Deshmukh R., Niederberger M., Mechanistic aspects in the formation, growth and surface functionalization of metal oxide nanoparticles in organic solvents, Chemistry—A European Journal, 23 (2017) 8542–8570. DOI: 10.1002/chem.201605957

Devarepally K.K., Cox D.C., Fry A.T., Stolojan V., Curry R.J., Munz M., Synthesis of linear ZnO structures by a thermal decomposition method and their characterisation, Journal of Materials Science, 47 (2012) 1893–1901. DOI: 10.1007/s10853-011-5978-6

Djerdj I., Arčon D., Jagličić Z., Niederberger M., Nonaqueous synthesis of metal oxide nanoparticles: short review and doped titanium dioxide as case study for the preparation of transition metal-doped oxide nanoparticles, Journal of Solid State Chemistry, 181 (2008a) 1571–1581. DOI: 10.1016/j.jssc.2008.04.016

Djerdj I., Garnweitner G., Arčon D., Pregelj M., Jagličić Z., Niederberger M., Diluted magnetic semiconductors: Mn/Co-doped ZnO nanorods as case study, Journal of Materials Chemistry, 18 (2008b) 5208–5217. DOI: 10.1039/b808361d

Doxsee K.M., Chang R.C., Chen E., Myerson A.S., Huang D., Crystallization of solid-state materials in nonaqueous gels. 1. Silver Bromide, Journal of the American Chemical Society, 120 (1998) 585–586. DOI: 10.1021/ja9704343

Ellis B.L., Knauth P., Djenizian T., Three-dimensional self-supported metal oxides for advanced energy storage, Advanced Materials, 26 (2014) 3368–3397. DOI: 10.1002/adma.201306126

Fattakhova-Rohlfing D., Zaleska A., Bein T., Three-dimensional titanium dioxide nanomaterials, Chemical Reviews, 114 (2014) 9487–9558. DOI: 10.1021/cr500201c

Fleischmann S., Kamboj I., Augustyn V., Nanostructured transition metal oxides for electrochemical energy storage, in: Transition Metal Oxides for Electrochemical Energy Storage, Wiley-VCH, ISBN: 9783527344932, 2022, pp. 183–212. DOI: 10.1002/9783527817252.ch8

Garnweitner G., Antonietti M., Niederberger M., Nonaqueous synthesis of crystalline anatase nanoparticles in simple ketones and aldehydes as oxygen-supplying agents, Chemical Communications, 2005 (2005) 397–399. DOI: 10.1039/b414510k

Garnweitner G., Grote C., In situ investigation of molecular kinetics and particle formation of water-dispersible titania nanocrystals, Physical Chemistry Chemical Physics, 11 (2009) 3767–3774. DOI: 10.1039/b821973g

Garnweitner G., Tsedev N., Dierke H., Niederberger M., Benzylamines as versatile agents for the one-pot synthesis and highly ordered stacking of anatase nanoplatelets, European Journal of Inorganic Chemistry, 2008 (2008) 890–895. DOI: 10.1002/ejic.200700995

Gliech M., Görlin M., Gocyla M., Klingenhof M., Bergmann A., Selve S., Spöri C., Heggen M., Dunin-Borkowski R.E., Suntivich J., Strasser P., Solute incorporation at oxide–oxide interfaces explains how ternary mixed-metal oxide nanocrystals support element-specific anisotropic growth, Advanced Functional Materials, 30 (2020) 1909054. DOI: 10.1002/adfm.201909054

Görke M., Garnweitner G., Crystal engineering of nanomaterials: current insights and prospects, CrystEngComm, 23 (2021) 7916–7927. DOI: 10.1039/d1ce00601k

Grabs I.-M., Bradtmöller C., Menzel D., Garnweitner G., Formation mechanisms of iron oxide nanoparticles in different nonaqueous media, Crystal Growth and Design, 12 (2012) 1469–1475. DOI: 10.1021/cg201563h

Hofmann C., Rusakova I., Ould-Ely T., Prieto-Centurión D., Hartman K.B., Kelly A.T., Lüttge A., Whitmire K.H., Shape control of new Fe_xO-Fe_3O_4 and $Fe_{1-y}Mn_yO$-$Fe_{3-z}Mn_zO_4$ nanostructures, Advanced Functional Materials, 18 (2008) 1661–1667. DOI: 10.1002/adfm.200701119

Hudry D., Apostolidis C., Walter O., Gouder T., Courtois E., Kübel C., Meyer D., Non-aqueous synthesis of isotropic and anisotropic actinide oxide nanocrystals, Chemistry—A European Journal, 18 (2012) 8283–8287. DOI: 10.1002/chem.201200513

Jia H., Zheng Z., Zhao H., Zhang L., Zou Z., Nonaqueous sol-gel synthesis and growth mechanism of single crystalline TiO_2 nanorods with high photocatalytic activity, Materials Research Bulletin, 44 (2009) 1312–1316. DOI: 10.1016/j.materresbull.2008.12.016

Joo J., Kwon S.G., Yu J.H., Hyeon T., Synthesis of ZnO nanocrystals with cone, hexagonal cone, and rod shapes via non-hydrolytic ester elimination sol-gel reactions, Advanced Materials, 17 (2005a) 1873–1877. DOI: 10.1002/adma.200402109

Joo J., Kwon S.G., Yu T., Cho M., Lee J., Yoon J., Hyeon T., Large-scale synthesis of TiO_2 nanorods via nonhydrolytic sol-gel ester elimina-

tion reaction and their application to photocatalytic inactivation of E. coli, Journal of Physical Chemistry B, 109 (2005b) 15297–15302. DOI: 10.1021/jp052458z

Jun Y., Choi J., Cheon J., Shape control of semiconductor and metal oxide nanocrystals through nonhydrolytic colloidal routes, Angewandte Chemie International Edition, 45 (2006) 3414–3439. DOI: 10.1002/anie.200503821

Jun Y.W., Casula M.F., Sim J.H., Kim S.Y., Cheon J., Alivisatos A.P., Surfactant-assisted elimination of a high energy facet as a means of controlling the shapes of TiO_2 nanocrystals, Journal of the American Chemical Society, 125 (2003) 15981–15985. DOI: 10.1021/ja0369515

Kachynski A.V., Kuzmin A.N., Nyk M., Roy I., Prasad P.N., Zinc oxide nanocrystals for nonresonant nonlinear optical microscopy in biology and medicine, Journal of Physical Chemistry C, 112 (2008) 10721–10724. DOI: 10.1021/jp801684j

Khokhra R., Singh R.K., Kumar R., Effect of synthesis medium on aggregation tendencies of ZnO nanosheets and their superior photocatalytic performance, Journal of Materials Science, 50 (2015) 819–832. DOI: 10.1007/s10853-014-8642-0

Kim C.S., Moon B.K., Park J.H., Choi B.C., Seo H.J., Solvothermal synthesis of nanocrystalline TiO_2 in toluene with surfactant, Journal of Crystal Growth, 257 (2003) 309–315. DOI: 10.1016/S0022-0248(03)01468-4

Kim D.H., Min K.-M., Park K.-S., Park I.J., Cho I.S., Seong W.M., Kim D.-W., Hong K.S., Controlled synthesis and Li-electroactivity of rutile TiO_2 nanostructure with walnut-like morphology, Dalton Transactions, 42 (2013) 4278–4284. DOI: 10.1039/c2dt32251j

Kolodziejczak-Radzimska A., Jesionowski T., Zinc oxide-from synthesis to application: a review, Materials, 7 (2014) 2833–2881. DOI: 10.3390/ma7042833

Koo B., Park J., Kim Y., Choi S.H., Sung Y.E., Hyeon T., Simultaneous phase- and size-controlled synthesis of TiO_2 nanorods via non-hydrolytic sol-gel reaction of syringe pump delivered precursors, Journal of Physical Chemistry B, 110 (2006) 24318–24323. DOI: 10.1021/jp065372u

Kovalenko M.V., Bodnarchuk M.I., Lechner R.T., Hesser G., Schäffler F., Heiss W., Fatty acid salts as stabilizers in size- and shape-controlled nanocrystal synthesis: the case of inverse spinel iron oxide, Journal of the American Chemical Society, 129 (2007) 6352–6353. DOI: 10.1021/ja0692478

Koziej D., Fischer F., Kränzlin N., Caseri W.R., Niederberger M., Nonaqueous TiO_2 nanoparticle synthesis: a versatile basis for the fabrication of self-supporting, transparent, and UV-absorbing composite films, ACS Applied Materials and Interfaces, 1 (2009) 1097–1104. DOI: 10.1021/am9000584

Kunjara Na Ayudhya S., Tonto P., Mekasuwandumrong O., Pavarajarn V., Praserthdam P., Solvothermal synthesis of ZnO with various aspect ratios using organic solvents, Crystal Growth & Design, 6 (2006) 2446–2450. DOI: 10.1021/cg050345z

Kwon S.G., Piao Y., Park J., Angappane S., Jo Y., Hwang N.-M., Park J.-G., Hyeon T., Kinetics of monodisperse iron oxide nanocrystal formation by "heating-up" process, Journal of the American Chemical Society, 129 (2007) 12571–12584. DOI: 10.1021/ja074633q

Lee E.J.H., Ribeiro C., Longo E., Leite E.R., Oriented attachment: an effective mechanism in the formation of anisotropic nanocrystals, Journal of Physical Chemistry B, 109 (2005) 20842–20846. DOI: 10.1021/jp0532115

Lee K., Seo W.S., Park J.T., Synthesis and optical properties of colloidal tungsten oxide nanorods, Journal of the American Chemical Society, 125 (2003) 3408–3409. DOI: 10.1021/ja034011e

Leite E.R., Giraldi T.R., Pontes F.M., Longo E., Beltrán A., Andrés J., Crystal growth in colloidal tin oxide nanocrystals induced by coalescence at room temperature, Applied Physics Letters, 83 (2003) 1566–1568. DOI: 10.1063/1.1605241

Li X.L., Peng Q., Yi J.X., Wang X., Li Y., Near monodisperse TiO_2 nanoparticles and nanorods, Chemistry—A European Journal, 12 (2006) 2383–2391. DOI: 10.1002/chem.200500893

Liu G., Yang H.G., Pan J., Yang Y.Q., Lu G.Q.M., Cheng H.-M., Titanium dioxide crystals with tailored facets, Chemical Reviews, 114 (2014) 9559–9612. DOI: 10.1021/cr400621z

Liu J.F., Bei Y.Y., Wu H.P., Shen D., Gong J.Z., Li X.G., Wang Y.W., Jiang N.P., Jiang J.Z., Synthesis of relatively monodisperse ZnO nanocrystals from a precursor zinc 2,4-pentanedionate, Materials Letters, 61 (2007) 2837–2840. DOI: 10.1016/j.matlet.2007.03.028

Ludi B., Süess M.J., Werner I.A., Niederberger M., Mechanistic aspects of molecular formation and crystallization of zinc oxide nanoparticles in benzyl alcohol, Nanoscale, 4 (2012) 1982–1995. DOI: 10.1039/c1nr11557j

Manna L., Scher E.C., Alivisatos A.P., Synthesis of soluble and processable rod-, arrow-, teardrop-, and tetrapod-shaped CdSe nanocrystals, Journal of the American Chemical Society, 122 (2000) 12700–12706. DOI: 10.1021/ja003055+

Masthoff I.C., Gutsche A., Nirschl H., Garnweitner G., Oriented attachment of ultra-small $Mn_{(1-x)}ZnxFe_2O_4$ nanoparticles during the non-aqueous sol-gel synthesis, CrystEngComm, 17 (2015) 2464–2470. DOI: 10.1039/c4ce02068e

Masthoff I.C., Kraken M., Mauch D., Menzel D., Munevar J.A., Baggio Saitovitch E., Litterst F.J., Garnweitner G., Study of the growth process of magnetic nanoparticles obtained via the non-aqueous sol-gel method, Journal of Materials Science, 49 (2014) 4705–4714. DOI: 10.1007/s10853-014-8160-0

Mutin P.H., Vioux A., Nonhydrolytic processing of oxide-based materials: simple routes to control homogeneity, morphology, and nanostructure, Chemistry of Materials, 21 (2009) 582–596. DOI: 10.1021/cm802348c

Mutin P.H., Vioux A., Recent advances in the synthesis of inorganic materials via non-hydrolytic condensation and related low-temperature routes, Journal of Materials Chemistry A, 1 (2013) 11504–11512. DOI: 10.1039/c3ta12058a

Niederberger M., Bartl M.H., Stucky G.D., Benzyl alcohol and titanium tetrachloride-a versatile reaction system for the nonaqueous and low-temperature preparation of crystalline and luminescent titania nanoparticles, Chemistry of Materials, 14 (2002a) 4364–4370. DOI: 10.1021/cm021203k

Niederberger M., Bartl M.H., Stucky G.D., Benzyl alcohol and transition metal chlorides as a versatile reaction system for the nonaqueous and low-temperature synthesis of crystalline nano-objects with controlled dimensionality, Journal of the American Chemical Society, 124 (2002b) 13642–13643. DOI: 10.1021/ja027115i

Niederberger M., Garnweitner G., Organic reaction pathways in the nonaqueous synthesis of metal oxide nanoparticles, Chemistry—A European Journal, 12 (2006) 7282–7302. DOI: 10.1002/chem.200600313

Niederberger M., Pinna N., Metal Oxide Nanoparticles in Organic Solvents—Synthesis, Formation, Assembly and Application, Springer London, London, 2009, ISBN: 9781848826700. DOI: 10.1007/978-1-84882-671-7

Nikam A.V., Prasad B.L.V., Kulkarni A.A., Wet chemical synthesis of metal oxide nanoparticles: a review, CrystEngComm, 20 (2018) 5091–5107. DOI: 10.1039/C8CE00487K

Ohayon E., Gedanken A., The application of ultrasound radiation to the synthesis of nanocrystalline metal oxide in a non-aqueous solvent, Ultrasonics Sonochemistry, 17 (2010) 173–178. DOI: 10.1016/j.ultsonch.2009.05.015

Pacholski C., Kornowski A., Weller H., Self-assembly of ZnO: from nanodots to nanorods, Angewandte Chemie International Edition, 41 (2002) 1188–1191. DOI: 10.1002/1521-3773(20020402)41:7<1188::AID-ANIE1188>3.0.CO;2-5

Palchoudhury S., An W., Xu Y., Qin Y., Zhang Z., Chopra N., Holler R.A.,

Turner C.H., Bao Y., Synthesis and growth mechanism of iron oxide nanowhiskers, Nano Letters, 11 (2011a) 1141–1146. DOI: 10.1021/nl200136j

Palchoudhury S., Xu Y., Goodwin J., Bao Y., Synthesis of iron oxide nanoworms, Journal of Applied Physics, 109 (2011b) 07E314. DOI: 10.1063/1.3549600

Panchakarla L.S., Govindaraj A., Rao C.N.R., Formation of ZnO nanoparticles by the reaction of zinc metal with aliphatic alcohols, Journal of Cluster Science, 18 (2007) 660–670. DOI: 10.1007/s10876-007-0129-6

Parashar M., Shukla V.K., Singh R., Metal oxides nanoparticles via sol–gel method: a review on synthesis, characterization and applications, Journal of Materials Science: Materials in Electronics, 31 (2020) 3729–3749. DOI: 10.1007/s10854-020-02994-8

Park J., An K., Hwang Y., Park J.-G., Noh H.-J., Kim J.-Y., Park J.-H., Hwang N.-M., Hyeon T., Ultra-large-scale syntheses of monodisperse nanocrystals, Nature Materials, 3 (2004a) 891–895. DOI: 10.1038/nmat1251

Park J., Kang E., Bae C.J., Park J.-G., Noh H.-J., Kim J.-Y., Park J.-H., Park H.M., Hyeon T., Synthesis, characterization, and magnetic properties of uniform-sized MnO nanospheres and nanorods, Journal of Physical Chemistry B, 108 (2004b) 13594–13598. DOI: 10.1021/jp048229e

Patzke G.R., Krumeich F., Nesper R., Oxidic nanotubes and nanorods—anisotropic modules for a future nanotechnology, Angewandte Chemie International Edition, 41 (2002) 2446–2461. DOI: 10.1002/1521-3773(20020715)41:14<2446::AID-ANIE2446>3.0.CO;2-K.

Peng Z.A., Peng X., Nearly monodisperse and shape-controlled CdSe nanocrystals via alternative routes: nucleation and growth, Journal of the American Chemical Society, 124 (2002) 3343–3353. DOI: 10.1021/ja0173167

Pinna N., Garnweitner G., Beato P., Niederberger M., Antonietti M., Synthesis of yttria-based crystalline and lamellar nanostructures and their formation mechanism, Small, 1 (2005) 112–121. DOI: 10.1002/smll.200400014

Pinna N., Karmaoui M., Willinger M.-G., The "benzyl alcohol route": an elegant approach towards doped and multimetal oxide nanocrystals: Short review and $ZnAl_2O_4$ nanostructures by oriented attachment, Journal of Sol-Gel Science and Technology, 57 (2011) 323–329. DOI: 10.1007/s10971-009-2111-2

Pinna N., Niederberger M., Surfactant-free nonaqueous synthesis of metal oxide nanostructures, Angewandte Chemie International Edition, 47 (2008) 5292–5304. DOI: 10.1002/anie.200704541

Polleux J., Gurlo A., Barsan N., Weimar U., Antonietti M., Niederberger M., Template-free synthesis and assembly of single-crystalline tungsten oxide nanowires and their gas-sensing properties, Angewandte Chemie International Edition, 45 (2006) 261–265. DOI: 10.1002/anie.200502823

Polleux J., Pinna N., Antonietti M., Niederberger M., Growth and assembly of crystalline tungsten oxide nanostructures assisted by bioligation, Journal of the American Chemical Society, 127 (2005) 15595–15601. DOI: 10.1021/ja0544915

Pucci A., Willinger M.-G., Liu F., Zeng X., Rebuttini V., Clavel G., Bai X., Ungar G., Pinna N., One-step synthesis and self-assembly of metal oxide nanoparticles into 3D superlattices, ACS Nano, 6 (2012) 4382–4391. DOI: 10.1021/nn3010735

Qamar M., Adam A., Azad A.-M., Kim Y.-W., Benzyl alcohol-mediated versatile method to fabricate nonstoichiometric metal oxide nanostructures, ACS Applied Materials and Interfaces, 9 (2017) 40573–40579. DOI: 10.1021/acsami.7b09515

Rai P., Kwak W.K., Yu Y.T., Solvothermal synthesis of ZnO nanostructures and their morphology-dependent gas-sensing properties, ACS Applied Materials and Interfaces, 5 (2013) 3026–3032. DOI: 10.1021/am302811h

Ramya M., Nideep T.K., Nampoori V.P.N., Kailasnath M., Understanding the role of alcohols in the growth behaviour of ZnO nanostructures prepared by solution based synthesis and their application in solar cells, New Journal of Chemistry, 43 (2019) 17980–17990. DOI: 10.1039/c9nj03212f

Redl F.X., Black C.T., Papaefthymiou G.C., Sandstrom R.L., Yin M., Zeng H., Murray C.B., O'Brien S.P., Magnetic, electronic, and structural characterization of nonstoichiometric iron oxides at the nanoscale, Journal of the American Chemical Society, 126 (2004) 14583–14599. DOI: 10.1021/ja046808r

Ribeiro C., Lee E.J.H., Longo E., Leite E.R., A Kinetic model to describe nanocrystal growth by the oriented attachment mechanism, ChemPhysChem, 6 (2005) 690–696. DOI: 10.1002/cphc.200400505

Ribeiro C., Lee E.J.H., Longo E., Leite E.R., Oriented attachment mechanism in anisotropic nanocrystals: a "polymerization" approach, ChemPhysChem, 7 (2006) 664–670. DOI: 10.1002/cphc.200500508

Sajanlal P.R., Sreeprasad T.S., Samal A.K., Pradeep T., Anisotropic nanomaterials: structure, growth, assembly, and functions, Nano Reviews, 2 (2011) 5883. DOI: 10.3402/nano.v2i0.5883

Šarić A., Despotović I., Štefanić G., Alcoholic solvent influence on ZnO synthesis: a joint experimental and theoretical study, Journal of Physical Chemistry C, 123 (2019) 29394–29407. DOI: 10.1021/acs.jpcc.9b07411

Satapathy S., Ahlawat A., Paliwal A., Singh R., Singh M.K., Gupta P.K., Effect of calcination temperature on nanoparticle morphology and its consequence on optical properties of Nd:Y_2O_3 transparent ceramics, CrystEngComm, 16 (2014) 2723–2731. DOI: 10.1039/c3ce42529k

Shavel A., Rodríguez-González B., Pacifico J., Spasova M., Farle M., Liz-Marzán L.M., Shape control in iron oxide nanocrystal synthesis, induced by trioctylammonium ions, Chemistry of Materials, 21 (2009) 1326–1332. DOI: 10.1021/cm803201p

Siddiqui M.R.H., Al-Wassil A.I., Al-Otaibi A.M., Mahfouz R.M., Effects of precursor on the morphology and size of ZrO_2 nanoparticles, synthesized by sol-gel method in non-aqueous medium, Materials Research, 15 (2012) 986–989. DOI: 10.1590/S1516-14392012005000128

Stolzenburg P., Freytag A., Bigall N.C., Garnweitner G., Fractal growth of ZrO_2 nanoparticles induced by synthesis conditions, CrystEngComm, 18 (2016) 8396–8405. DOI: 10.1039/c6ce01916a

Styskalik A., Skoda D., Barnes C.E., Pinkas J., The power of non-hydrolytic sol-gel chemistry: a review, Catalysts, 7 (2017) 168. DOI: 10.3390/catal7060168

Su H., Jaffer S., Yu H., Transition metal oxides for sodium-ion batteries, Energy Storage Materials, 5 (2016) 116–131. DOI: 10.1016/j.ensm.2016.06.005

Teja A.S., Koh P.-Y., Synthesis, properties, and applications of magnetic iron oxide nanoparticles, Progress in Crystal Growth and Characterization of Materials, 55 (2009) 22–45. DOI: 10.1016/j.pcrysgrow.2008.08.003

Tonto P., Mekasuwandumrong O., Phatanasri S., Pavarajarn V., Praserthdam P., Preparation of ZnO nanorod by solvothermal reaction of zinc acetate in various alcohols, Ceramics International, 34 (2008) 57–62. DOI: 10.1016/j.ceramint.2006.08.003

Ungerer J., Thurm A.-K., Garnweitner G., Nirschl H., Formation of aluminum-doped zinc oxide nanocrystals via the benzylamine route at low reaction kinetics, Chemical Engineering and Technology, 43 (2020) 797–803. DOI: 10.1002/ceat.201900466

Ungerer J., Thurm A.-K., Meier M., Klinge M., Garnweitner G., Nirschl H., Development of a growth model for aluminum-doped zinc oxide nanocrystal synthesis via the benzylamine route, Journal of Nanoparticle Research, 21 (2019) 106. DOI: 10.1007/s11051-019-4547-9

Védrine J.C., Heterogeneous catalysis on metal oxides, Catalysts, 7 (2017) 341. DOI: 10.3390/catal7110341

Venkatesan A., Krishna Chandar N.R., Kandasamy A., Karl Chinnu M., Marimuthu K.N., Mohan Kumar R., Jayavel R., Luminescence and electrochemical properties of rare earth (Gd, Nd) doped V_2O_5 nano-

structures synthesized by a non-aqueous sol-gel route, RSC Advances, 5 (2015) 21778–21785. DOI: 10.1039/c4ra14542a

Voigt M., Klaumünzer M., Thiem H., Peukert W., Detailed analysis of the growth kinetics of ZnO nanorods in methanol, Journal of Physical Chemistry C, 114 (2010) 6243–6249. DOI: 10.1021/jp911258d

Wang C., Deng Z.X., Li Y., The synthesis of nanocrystalline anatase and rutile titania in mixed organic media, Inorganic Chemistry, 40 (2001) 5210–5214. DOI: 10.1021/ic0101679

Wang C., Deng Z., Zhang G., Fan S., Li Y., Synthesis of nanocrystalline TiO_2 in alcohols, Powder Technology, 125 (2002) 39–44. DOI: 10.1016/S0032-5910(01)00523-X

Wang C., Shen E., Wang E., Gao L., Kang Z., Tian C., Lan Y., Zhang C., Controllable synthesis of ZnO nanocrystals via a surfactant-assisted alcohol thermal process at a low temperature, Materials Letters, 59 (2005) 2867–2871. DOI: 10.1016/j.matlet.2005.04.031

Wang H., Xin L., Wang Hai, Yu X., Liu Y., Zhou X., Li B., Aggregation-induced growth of hexagonal ZnO hierarchical mesocrystals with interior space: nonaqueous synthesis, growth mechanism, and optical properties, RSC Advances, 3 (2013) 6538–6544. DOI: 10.1039/c3ra23010d

Woo K., Hong J., Ahn J.-P., Park J.-K., Kim K.-J., Coordinatively induced length control and photoluminescence of $W_{18}O_{49}$ nanorods, Inorganic Chemistry, 44 (2005) 7171–7174. DOI: 10.1021/ic0504644

Wu B., Guo C., Zheng N., Xie Z., Stucky G.D., Nonaqueous production of nanostructured anatase with high-energy facets, Journal of the American Chemical Society, 130 (2008) 17563–17567. DOI: 10.1021/ja8069715

Wu Y., Liu H.-M., Xu B.-Q., Solvothermal synthesis of TiO_2: anatase nanocrystals and rutile nanofibres from $TiCl_4$ in acetone, Applied Organometallic Chemistry, 21 (2007a) 146–149. DOI: 10.1002/aoc.1184

Wu Y., Liu H.-M., Xu B.-Q., Zhang Z.-L., Su D.-S., Single-phase titania nanocrystallites and nanofibers from titanium tetrachloride in acetone and other ketones, Inorganic Chemistry, 46 (2007b) 5093–5099. DOI: 10.1021/ic070199h

Xu L., Hu Y.-L., Pelligra C., Chen C.-H., Jin L., Huang H., Sithambaram S., Aindow M., Joesten R., Suib S.L., ZnO with different morphologies synthesized by solvothermal methods for enhanced photocatalytic activity, Chemistry of Materials, 21 (2009) 2875–2885. DOI: 10.1021/cm900608d

Xue X., Penn R.L., Leite E.R., Huang F., Lin Z., Crystal growth by oriented attachment: kinetic models and control factors, CrystEngComm, 16 (2014) 1419–1429. DOI: 10.1039/c3ce42129e

Yang Y., Yao Y., He L., Zhong Y., Ma Y., Yao J., Nonaqueous synthesis of TiO_2-carbon hybrid nanomaterials with enhanced stable photocatalytic hydrogen production activity, Journal of Materials Chemistry A, 3 (2015) 10060–10068. DOI: 10.1039/c5ta00638d

Yin M., Gu Y., Kuskovsky I.L., Andelman T., Zhu Y., Neumark G.F., O'Brien S., Zinc oxide quantum rods, Journal of the American Chemical Society, 126 (2004) 6206–6207. DOI: 10.1021/ja031696+

Yu H.X., Guo C.Y., Zhang X.F., Xu Y.M., Cheng X.L., Gao S., Huo L.H., Recent development of hierarchical metal oxides based gas sensors: from gas sensing performance to applications, Advanced Sustainable Systems, 6 (2022) 2100370. DOI: 10.1002/adsu.202100370

Yu X., Marks T.J., Facchetti A., Metal oxides for optoelectronic applications, Nature Materials, 15 (2016) 383–396. DOI: 10.1038/nmat4599

Yuhas B.D., Zitoun D.O., Pauzauskie P.J., He R., Yang P., Transition-metal doped zinc oxide nanowires, Angewandte Chemie International Edition, 45 (2006) 420–423. DOI: 10.1002/anie.200503172

Zellmer S., Kockmann A., Dosch I., Temel B., Garnweitner G., Aluminum zinc oxide nanostructures with customized size and shape by non-aqueous synthesis, CrystEngComm, 17 (2015) 6878–6883. DOI: 10.1039/c5ce00629e

Zhang L., Dou Y.-H., Gu H.-C., Sterically induced shape control of magnetite nanoparticles, Journal of Crystal Growth, 296 (2006) 221–226. DOI: 10.1016/j.jcrysgro.2006.08.010

Zhang W.-D., Xiao H.-M., Zhu L.-P., Fu S.-Y., Template-free solvothermal synthesis and magnetic properties of novel single-crystalline magnetite nanoplates, Journal of Alloys and Compounds, 477 (2009) 736–738. DOI: 10.1016/j.jallcom.2008.10.105

Zhang Y.-L., Li X.-F., Containing manganese DMSs nanostructures via a nonaqueous route, Advanced Materials Research, 79–82 (2009) 533–536. DOI: 10.4028/www.scientific.net/AMR.79-82.533

Zhang Y., Nayak T.R., Hong H., Cai W., Biomedical applications of zinc oxide nanomaterials, Current Molecular Medicine, 13 (2013) 1633–1645. DOI: 10.2174/15665240130666131111130058

Zhang Z., Liu S., Chow S., Han M.Y., Modulation of the morphology of ZnO nanostructures via aminolytic reaction: from nanorods to nanosquamas, Langmuir, 22 (2006) 6335–6340. DOI: 10.1021/la060351c

Zhang Z., Lu M., Xu H., Chin W.S., Shape-controlled synthesis of zinc oxide: a simple method for the preparation of metal oxide nanocrystals in non-aqueous medium, Chemistry—A European Journal, 13 (2007) 632–638. DOI: 10.1002/chem.200600293

Zhang Z., Zhong X., Liu S., Li D., Han M., Aminolysis route to monodisperse titania nanorods with tunable aspect ratio, Angewandte Chemie, 117 (2005) 3532–3536. DOI: 10.1002/ange.200500410

Zhao Z.-G., Miyauchi M., Nanoporous-walled tungsten oxide nanotubes as highly active visible-light-driven photocatalysts, Angewandte Chemie International Edition, 47 (2008) 7051–7055. DOI: 10.1002/anie.200802207

Zhao Z.G., Miyauchi M., Shape modulation of tungstic acid and tungsten oxide hollow structures, Journal of Physical Chemistry C, 113 (2009) 6539–6546. DOI: 10.1021/jp900160u

Zhao Z., Wang Y., Delmas C., Mingotaud C., Marty J.D., Kahn M.L., Mechanistic insights into the anisotropic growth of ZnO nanoparticles deciphered through 2D size plots and multivariate analysis, Nanoscale Advances, 3 (2021) 6696–6703. DOI: 10.1039/d1na00591j

Zhong X., Feng Y., Zhang Y., Lieberwirth I., Knoll W., Nonhydrolytic alcoholysis route to morphology-controlled ZnO nanocrystals, Small, 3 (2007) 1194–1199. DOI: 10.1002/smll.200600684

Zhong X., Knoll W., Morphology-controlled large-scale synthesis of ZnO nanocrystals from bulk ZnO, Chemical Communications, (2005) 1158–1160. DOI: 10.1039/b414948c

Zhong X., Xie R., Sun L., Lieberwirth I., Knoll W., Synthesis of dumbbell-shaped manganese oxide nanocrystals, The Journal of Physical Chemistry B, 110 (2006) 2–4. DOI: 10.1021/jp056064j

Zhou Z., Zhu X., Wu D., Chen Q., Huang D., Sun C., Xin J., Ni K., Gao J., Anisotropic shaped iron oxide nanostructures: controlled synthesis and proton relaxation shortening effects, Chemistry of Materials, 27 (2015) 3505–3515. DOI: 10.1021/acs.chemmater.5b00944

Zitoun D., Pinna N., Frolet N., Belin C., Single crystal manganese oxide multipods by oriented attachment, Journal of the American Chemical Society, 127 (2005) 15034–15035. DOI: 10.1021/ja0555926

Authors' Short Biographies

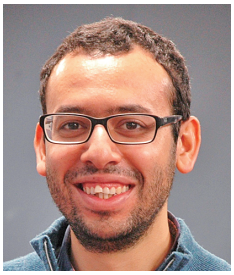

Sherif Okeil

Sherif Okeil is currently working as a competence team leader for nanomaterial synthesis in Georg Garnweitner's group at the Institute for Particle Technology, Technical University of Braunschweig. He received his bachelor's degree in Pharmacy at Ain Shams University in Cairo, Egypt in 2009. In 2013, he obtained his masters in Pharmaceutical Analytical Chemistry from the same university. In 2014, he was awarded a scholarship from the German Academic Exchange Service (DAAD) through which he obtained his Ph.D. in Inorganic Chemistry at the Technical University of Darmstadt in 2020. His current research interests are inorganic nanomaterial synthesis and their electronic applications.

Julian Ungerer

Julian Ungerer obtained his bachelor's degree in applied mechanics in 2013 and his master's degree in the process engineering machines group of Prof. Dr.-Ing Hermann Nirschl at the Karlsruhe Institute of Technology in 2016, where he also continued his academic research in the field of functional nanomaterials for renewable energy systems before receiving his Ph.D. in 2022.

Hermann Nirschl

Hermann Nirschl received his Ph.D. in Fluid Mechanics from the Technical University of Munich in 1994. For his habilitation in 1997 he worked on the numerical simulation of the particle-laden flows. He entered the 3M company in the dental division as the head of process engineering in the years between 1997 and 2002 where he worked as a project manager for different projects in Munich and St. Paul/Minnesota. Since 2003 he is Professor for Mechanical Process Engineering at the KIT in Karlsruhe. The focus of the research is on particle technology with a special emphasis on separation processes, numerical simulations and the development of particle analysis technologies.

Georg Garnweitner

Georg Garnweitner received a Diploma in Technical Chemistry at Vienna University of Technology, Austria, in 2003 and then moved to the Max Planck Institute of Colloids and Interfaces, Potsdam, Germany, where he obtained his Ph.D. in Colloids Chemistry in 2005. He was appointed as Professor at Technische Universität Braunschweig, Germany, in 2007. His research is centered on the synthesis of inorganic nanoparticles and hybrid materials, in particular via nonaqueous approaches. In addition, the surface modification and functionalization of nanomaterials are studied in his group, targeting diverse application fields such as solid-state and lithium-sulfur batteries, lightweight composites and drug delivery.